DEVELOPMENT OF TUNGSTEN LOADED AND ZIRCONIA INCORPORATED MESOPOROUS CATALYSTS FOR ESTERIFICATION OF PALMITIC ACID WITH CETYL ALCOHOL

A Thesis Submitted to
The Graduate School of Engineering and Sciences of
İzmir Institute of Technology
In Partial Fulfillment of the Requirements for the Degree of

MASTER OF SCIENCE

in Material Science and Engineering

by
Vahide Nuran MUTLU

June 2014
İZMİR

We approve the thesis of **Vahide Nuran MUTLU**

Examining Committee Members:

_____
Prof. Dr. Selahattin YILMAZ
Department of Chemical Engineering, Izmir Institute of Technology

_____
Prof. Dr. Seher Fehime ÖZKAN
Department of Chemical Engineering, Izmir Institute of Technology

_____
Assoc. Prof. Dr. Nuray OKTAR
Department of Chemical Engineering, Gazi University

16 June 2014

_____
Prof. Dr. Selahattin YILMAZ
Supervisor, Department of Chemical
Enginnering,Izmir Institute of
Technology

_____   _____
Assoc. Prof.Dr. Mustafa M. DEMİR   **Prof. Dr. R. Tuğrul SENGER**
Head of the Department of Material   Dean of the Graduate School of Engineering
Science and Engineering   and Sciences

ACKNOWLEDGEMENTS

ABSTRACT

DEVELOPMENT OF TUNGSTEN LOADED AND ZIRCONIA INCORPORATED MESOPOROUS CATALYSTS FOR ESTERIFICATION OF PALMITIC ACID WITH CETYL ALCOHOL

In this study, it was pursued to develop acidic mesoporous catalysts for esterification of cetyl alcohol by palmitic acid. For this, Zr incorporated SBA-15 was prepared by hydrothermal synthesis. Zr-SBA-15 was used both as a catalyst support and as a catalyst itself. WO_3 loading onto the Zr-SBA-15 was performed by incipient wetness impregnation. Additionally, WO_3-ZrO_2 catalyst was prepared by co-precipitation with two different contents of WO_3 (15 wt% and 20 wt%). The reaction tests were carried out in mesitylene under reflux conditions.

Zr was incorporated into SBA-15 successfully. The surface areas of Zr-SBA-15 and WO_3/Zr-SBA-15 catalysts were significantly higher than that of WO_3-ZrO_2. Loading of WO_3 decreased the surface area of Zr-SBA-15. The acidity of the WO_3/Zr-SBA-15 with 15 wt% WO_3 was higher than that of with 20 wt% WO_3. Moreover, increasing the calcination temperature from 700 to 800 ^{o}C resulted in the increase of acidity.

The activity of the catalysts differed. The only product obtained was cetyl palmitate. Under the test conditions it was found that the reaction rate was not limited by equilibrium. Zr-SBA-15 provided the highest conversion (64 %) which corresponded to cetyl palmitate yield of 63% among other mesoporous catalysts because of its high surface area (600.3 m^2/g) and acidity (0.152 mmol NH_3/g cat). This catalyst did not show leaching. WO_3/Zr-SBA-15 based catalys tests showed that catalyst activity increased by increasing calcination temperature. This was atributed to better dispersion of W. The conversion of cetyl alcohol did not change much with more W loading.

ÖZET

PALMİTİK ASİTİN SETİL ALKOL İLE ESTERİFİKASYONU İÇİN TUNGSTEN YÜKLÜ ZİRKONYA İÇEREN MEZOGÖZENEKLİ KATALİZÖRLERİN GELİŞTİRİLMESİ

Bu çalışmada, setil alkolün palmitik asit ile esterifikasyonu için mezogözenekli asit katalizörlerin geliştirilmesi amaçlanmıştır. Bunun için hidrotermal sentez ile SBA-15 yapısına Zr yüklemesi yapılmıştır. Zr-SBA-15 hem katalizör hem de destek malzemesi olarak kullanılmıştır. Zr-SBA-15 üzerine iki farklı miktarda (kütlece % 15 ve % 20) WO_3 yüklemesi emdirme yöntemi kullanılarak yapılmıştır. Bu katalizörlerin iki farklı sıcaklıkta (700 ^{o}C and 800 ^{o}C) kalsine edilmesiyle kalsinasyon sıcaklığının etkisi incelenmiştir. Buna ek olarak, birlikte çöktürme metodu ile iki farkılı miktarda WO_3 içeriğine (kütlece % 15 ve % 20) sahip WO_3-ZrO_2 katalizörler hazırlanmıştır. Tepkimeler geri soğutmalı koşullarda yapılmıştır.

SBA-15 yapısına Zr başarılı şekilde eklenmiştir. Zr-SBA-15 ve WO_3/Zr-SBA-15 katalizörlerin yüzey alanları WO_3-ZrO_2 katalizörlerin yüzey alanlarından belirgin biçimde yüksek bulunmuştur. WO_3 yüklemesinin Zr-SBA-15 in yüzey alanını düşürdüğü görülmüştür. Kütlece % 15 WO_3 içeren WO_3/Zr-SBA-15 katalizörlerin asitliği kütlece % 20 WO_3 içerenlere göre daha yüksektir. Ayrıca, kalsinasyon sıcaklığının 700 den 800 ^{o}C ye arttırılması ile asitlikler artmıştır.

Katalizörler farklı aktiviteler göstermiştir. Elde edilen tek ürün setil palmitat olmuştur. Testlerde tepkimenin denge tarafından kısıtlanmadığı bulunmuştur. Zr-SBA-15 yüksek yüzey alanı (600.3 m^2/g) ve asitliği (0.152 mmol NH_3/g kat) nedeniyle, diğer mezogözenekli katalizörler arasında en yüksek dönüşümü (% 64) ve setil palmitat verimini (% 63) göstermiştir. Bu katalizör katıdan çözünerek bozulma göstermemiştir. WO_3/Zr-SBA-15 tabanlı katalizörler, aktivitenin kalsinasyon sıcaklığı ile arttığını göstermiştir. Bu sonuç daha iyi W dağılımına bağlanmıştır. W yükleme miktarı dönüşümü fazla değiştirmemiştir.

dedicated to

my husband; *Ümit MUTLU*

TABLE OF CONTENTS

LIST OF FIGURES

LIST OF TABLES

CHAPTER 1

INTRODUCTION

Fatty acid esters are used as raw materials for emulsifiers or as oiling agent for foods, spin finishes and textiles, lubricants for plastics, paint and ink additives and for mechanical processing, personal care emollients, surfactants and base materials for perfumes. They are also used as solvents, co-solvents, and oil carries in the agricultural industry. Fatty acid esters are produced by esterification of fatty acid and alcohols.

Cetyl esters are fatty acid esters of cetyl alcohol. They are commonly used cosmetic industry. Cetyl esters are currently used as a skin conditioning agent, emollient in over 200 cosmetic formulations at concentrations up to 7%. Cetyl esters wax offers an easy way to increase the viscosity of creams and lotions while also improving the feel. The esters that are found in cetyl esters include cetyl palmitate, cetyl stearate, myristyl myristate, and myristyl stearate. In our study cetyl palmitate which is one of the most important ester for cosmetic industry was produced by esterification of cetyl alcohol and palmitic acid.

Palmitic acid is a saturated fatty acid with the molecular formula as $CH_3(CH_2)_{14}CO_2H$. It is the most common fatty acid found in animals, plants and microorganisms. It is a major component of palm oil, palm kernel oil, and coconut oil. Cetyl alcohol, also known as 1-hexadecanol and palmityl alcohol, is a fatty alcohol with the formula $CH_3(CH_2)_{15}OH$. It is used as an emulsion stabilizer and opacifier in cosmetic industry.

Fatty acid esters are produced conventionally by the esterification of acids and alcohols using a mineral acids such as concentrated sulfuric acid as the catalyst. These catalysts suffer from inherent problems of corrosiveness, high susceptibility to water, difficulty in catalyst recovery, environmental hazards, and waste control (Mantri et al., 2005). It is therefore important to replace these hazardous and polluting acids with environmentally friendly catalysts, which are active under mild conditions, and which can be easily recovered and reused.

Catalysts studied in recent investigations include zeolites, acidic resins, sulfated zirconia, tungstated zirconia and heteropoly acids. However, the success of the catalysis was limited to esters less than C_{10} in either carboxylic acids or alcohols

(Mantri et al., 2007). Mesoporous silica supported catalysts were studied in the literature. The esterification of different fatty acids and fatty alcohols was studied over MCM-48 supported tungstophosphoric acid under supercritical conditions. These catalysts gave high ester yield but showed leaching problems (Sakthivel et al., 2008). Supported and unsupported multivalent metal salt hydrates were tested for the esterification of long chain fatty acids and fatty alcohols. Supporting the metal salt hydrates on ordered mesoporous silica surprisingly enhanced the catalytic activity of the esterification although the activities changed depending on type of salt hydrates (Mantri et al., 2007) .

Different types of solvents such as benzene, toluene, m-xylene, mesitylene, diethylbenzenes and tetralin were tested for the esterification of long chain fatty acids and fatty alcohols. The type of solvent determined the reaction temperature, since the reaction was performed at the boiling point of the solvent. The maximum yield of ester was obtained with tetralin at 207 ^{o}C. However, mesitylene was found as a promising solvent with a yield of 89.3 % and a boiling point of 162 ^{o}C (Mantri et al., 2005).

The studies in the literature investigated the reaction parameters such as reaction temperature, solvent type, and reactant ratio, while the effects of the catalyst preparation methods on the acidity and surface properties of the catalysts and on the yield of the esters were not examined in detail (Mantri et al., 2005; Mantri et al., 2007; Sakthivel et al., 2008; Ieda et al., 2008).

In this study, acidic mesoporous catalysts were prepared for esterification of cetyl alcohol by palmitic acid. For this, Zr incorporated SBA-15 was prepared by hydrothermal synthesis. Another catalyst was prepared by loading WO_3 by incipient wetness impregnation method on this material. Different loading amounts of WO_3 (15 wt% and 20 wt%) were pursued. The effect of calcination temperature was also investigated by calcining these catalysts at 700 ^{o}C and 800 ^{o}C. In addition, catalyst amount and reactant composition were investigated as a parameter.

CHAPTER 2

ESTERIFICATION

Esters are derived from carboxylic acids. A carboxylic acid contains the -COOH group, and in an ester the hydrogen in this group is replaced by a hydrocarbon group. Esters are common in organic chemistry and biological materials, and often have a characteristic pleasant, fruity odor. This leads to their extensive use in the fragrance and flavor industry. Esters are used as raw materials for emulsifiers or as oiling agents for foods, spin finishes and textiles; lubricants for plastics; paint and ink additives and for mechanical processing; personal care emollients; surfactants and base materials for perfumes. Ester bonds are also found in many polymers. Esterification is the general name for a chemical reaction in which two reactants (typically an alcohol and an acid) form an ester as the reaction product. There are different routes to produce esters.

Alcoholysis of acid chlorides, anhydrides, or nitriles is one of these routes. In this type of reactions, Alcohols react with acyl chlorides and acid anhydrides to give esters (March et al., 2001).

$$RCOCl + R'OH \rightarrow RCO_2R' + HCl$$

$$(RCO)_2O + R'OH \rightarrow RCO_2R' + RCO_2H$$
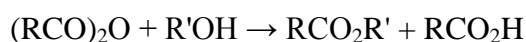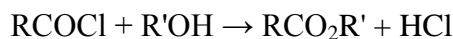
The reactions are irreversible simplifying work-up. Since acyl chlorides and acid anhydrides also react with water, anhydrous conditions are preferred. The analogous acylations of amines to give amides are less sensitive because amines are stronger nucleophiles and react more rapidly than does water. This method is employed only for laboratory-scale procedures, as it is expensive.

Another way to produce esters is transesterification, which involves changing one ester into another one. Like the hydrolysation, transesterification is catalysed by acids and bases. The reaction is widely used for degrading triglycerides, e.g. in the production of fatty acid esters and alcohols. (March et al., 2001).

$$RCO_2R' + CH_3OH \rightarrow RCO_2CH_3 + R'OH$$
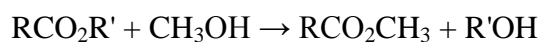
Alkenes undergo hydroesterification in the presence of metal carbonyl catalysts. Esters of propionic acid are produced commercially by this method:

$$C_2H_4 + ROH + CO \rightarrow C_2H_5CO_2R$$

The carbonylation of methanol yields methyl formate, which is the main commercial source of formic acid. The reaction is catalyzed by sodium methoxide:

$$CH_3OH + CO \rightarrow CH_3O_2CH$$
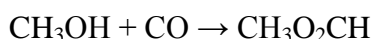
Although not widely employed for esterifications, salts of carboxylate anions can be alkylating agent with alkyl halides to give esters. In the case that an alkyl chloride is used, an iodide salt can catalyze the reaction (Finkelstein reaction).

The final and the most commonly used method to produce esters is the esterification of carboxylic acids with an alcohol in the presence of an acid catalyst. This reaction is also known as Fischer esterification. The mechanism of Fischer esterification is shown in Figure 2.1.
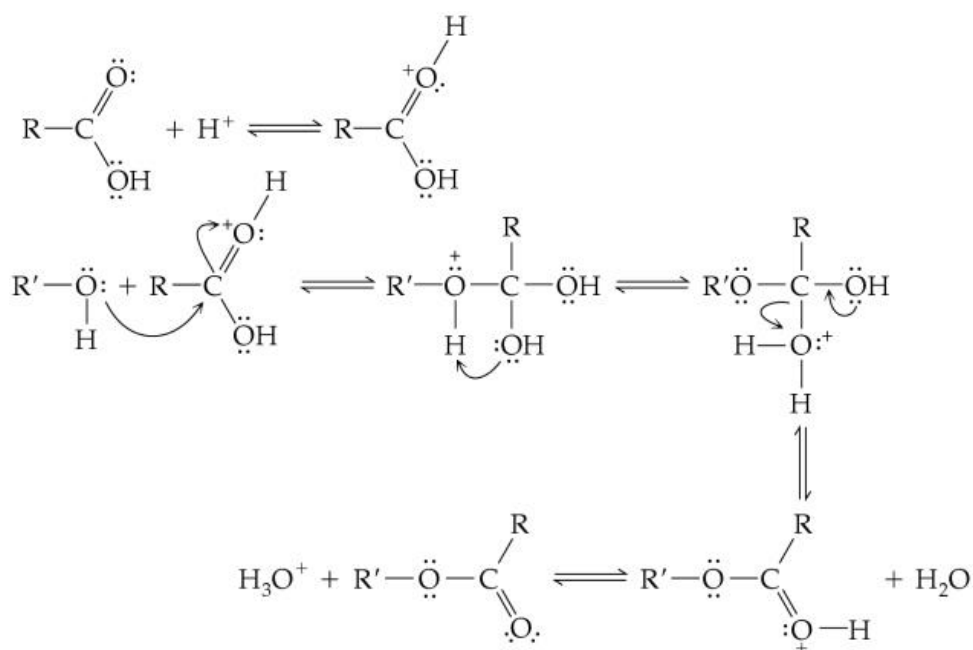
Figure 2.1. Fischer Esterification Mechanism
(Source : Mayo, Pike and Forbes 2010)

Fischer esterification reaction proceeds by nucleophilic attack of the alcohol on the protonated carbonyl group of the carboxylic acid to form a tetrahedral intermediate.

Collapse of the intermediate regenerates the carbonyl group and produces the ester and water (Mayo et al., 2010).

The primary advantages of Fischer esterification compared to other esterification processes are based on its relative simplicity. Straightforward acidic conditions can be used if acid sensitive functional groups are not an issue; sulfuric acid can be used; softer acids can be used with a tradeoff of longer reaction times. Because the reagents used are direct, there is less environmental impact in terms of waste products and harmfulness of the reagents. In other routes for ester production, alkyl halides are potential greenhouse gases or ozone depletors and possible ecological poisons. Acid chlorides evolve hydrochloric acid gas upon contact with atmospheric moisture, are corrosive, react vigorously with water and other nucleophiles sometimes dangerously; they are easily quenched by other nucleophiles besides the desired alcohol; their most common synthesis routes involve the evolution of toxic carbon monoxide or sulfur dioxide gases. Fischer esterification is primarily a thermodynamically controlled process: because of its slowness, the most stable ester tends to be the major product. This can be a desirable trait if there are multiple reaction sites and side product esters to be avoided. In contrast, rapid reactions involving acid anhydrides or acid chlorides are often kinetically controlled.

Esterification is an equilibrium reaction. The products of Fischer esterification are only slightly favored by the equilibrium. Therefore, the equilibrium must be shifted toward the product in order to obtain substantial yield of ester. This might be accomplished by the removal of one or both of the products (the ester or water).

The rate determining step of Fischer esterification is the formation of the tetrahedral intermediate. As a consequence, the rate of reaction will be determined by the ease with which the nucleophile (alcohol) approaches the carbonyl group. Steric and electronic factors have been shown to have large effects on the rate of esterification. Therefore, the chain length and branching of acid and alcohol is important for esterification. Mantri et al (2005) studied the esterfication of different long chain fatty acids and fatty alcohols. The results of the study showed that the yield of ester is increasing with decreasing the length of alcohols and acids.

Another important factor that effects the rate of esterification reaction is acid/alcohol mole ratio. Since the esterification is an equilibrium reaction, the equilibrium might be shifted towards the products by using excess reactant. Therefore, it is logical to use one of the reactants in excess amount by considering the

stoichiometry of the reaction. This method is commonly used to produce fatty acid methyl esters or fatty acid ethyl esters. Since alcohols like methanol and ethanol have reasonable costs and they are easier to be found, these alcohols are used in excess amounts for esterification. However, it is not a preffered method for the esterification of long chain fatty acids with long chain fatty alcohols, because both the acid and the alcohol used in these reactions are expensive reagents. Also it is not easy to seperate rhe product and the reactants. Thus, it is needed to develop active catalysts which can give high yields with equimolar reactant compositions.

The type of solvent used for the reaction and reaction temperature are the two factors that effect the reaction rate and yield. The esterification reaction is generally performed at azeotropic conditions in order to remove the water produced as the side product. For this reason, the reaction temperature is dependent on the solvent that is used in the reaction. Mantri et al (2005) investigated the effect of the solvent and reaction temperature on the yield of cetyl palmitate by testing different solvents having different boiling temperatures such as benzene (80°C), toluene (110°C), m-xylene (140°C), mesitylene (162°C), diethylbenzenes(182°C) and tetralin (207°C). It was observed that the yield of cetyl palmitate increased with reaction temperature depending on the boiling point of the solvent. The highest yield was obtained with tetralin as 100%, and then with diethylbenzenes as 99.6%, whereas the yield obtained with mesitylene was 86.2%. However, considering the industrial conditions , it is also important to be able to obtain high yield at reasonable reaction temperatures. Therefore, the most appliable solvent was decided to be mesitylene with comparable high yield and reasonable reaction temperature.

Another important factor on the rate of esterification is the amount of the catalysts used for the reaction, because it is desired to reduce the reaction time to achieve the expected yield of ester. Therefore, the amount of the catalysts was studied as a parameter in this study.

Esterification reaction occur without adding catalyst because of the weak acidity of carboxylic acids themselves, but the reaction is extremely slow and requires several days to get equilibrium at typical reaction condtions. For this reason, homogeneous catalysts, such as concentrated H_2SO_4 and HCl are used. However, these homogeneous acid catalysts suffer from several drawbacks, such as equipment corrosion, waste treatment, seperation and recycling of the catalyst. The use of a heterogeneous acid catalyst to replace the homogenous acid can eliminate these problems. Heterogenous

catalysts, such as ion exchange resin (Özbay et al., 2008) sulfonated cation exchange resin (Jiang et al., 2013), zeolites (Marchetti et al., 2008), sulfated zirconia (Ni et al., 2007) and heteropoly acids (Brahmkhatri et al., 2011) were studied for esterification reaction in the literature. However, the success of the catalysts was limited to esters less than 10 carbons in their carboxylic acids or alcohols. No promising method has been identified to esterify long chain carboxylic acids with long chain alcohols.

CHAPTER 3

LITERATURE SEARCH

Fatty acid esterification reactions are performed conventionally with mineral acids such as sulfuric acid, as the catalyst. However, homogeneous catalysts have disadvantages like corrosiveness, high susceptibility to water, difficulty in catalyst recovery, environmental hazards and waste control. Although the esterification of fatty acids has been studied also over heterogeneous catalysts such as supported heteropoly acids, sulphated zirconia, tungstated zirconia, the success of the catalysis was limited to esters less than 10 carbons in either acid or alcohols. There are limited studies about the esterification of long chain fatty acids with long chain fatty alcohols in the literature.

Mantri et al. (2005) studied the esterification of long chain fatty acid with long chain primary and secondary alcohols over $ZrOCl_2.8H_2O$ supported on mesoporous silica catalysts. They used different zirconyl salts such as chlorides, nitrates, sulfate and acetate for their investigations. The results showed that catalytic activity of these zirconyl salts was due to the zirconyl moiety and not the anion moiety. Zirconyl salts were loaded on different types of supports like mesoporous silicas (MCM-41, FSM-16, SBA-15), amorphous silica, alumina, zirconia and activated charcoal. It was observed that the mesoporous silica supports enhanced the catalytic activity significantly. The reason of this enhancement was the hydrophobic character of mesoporous silica supports which stabilizes the catalytic species and accelerates the removal of water.

The effect of solvent type on the yield of cetyl palmitate was also investigated by using different solvents having different boiling temperatures such as mesitylene (162 ^{o}C) , benzene (80 ^{o}C), toluene (110 ^{o}C), m-xylene (140 ^{o}C), diethylbenzenes (182 ^{o}C) and tetralin (207 ^{o}C). The result showed that the yield of cetyl palmitate increased with the reaction temperature. However, mesitylene was found as the most appliable solvent with high yield (86.2%) at reasonable reaction temperature. In this study the effect of $ZrOCl_2.8H_2O$ loading on MCM-41 was also examined. The cetyl palmitate yields obtained are given in Table 3.1. Loading was changed by altering the amount of MCM-41 at constant amounts of $ZrOCl_2.8H_2O$. The catalytic activity increased with high loading even with the same quantity of $ZrOCl_2.8H_2O$, the esterification was almost completed by loading more than 30 wt% $ZrOCl_2$ on MCM-41.

Table 3.1. Effect of loading of $ZrOCl_2.8H_2O$ on MCM-41 on the yield of cetyl palmitate (Source : Mantri et al., 2005)

Loading	Yield (%)
-	2.5
5	27.5
10	70.8
20	89.3
30	95.6
40	99.5

In another study by Mantri et al. (2007), the multivalent salt hydrates as catalyst were investigated for the esterification of fatty acids and alcohols.Among different metal salt hydrates Fe^{+3} , Al^{+3}, Ga^{+3} and $In^{+}3$ were the most effective catalyst for the reactions. Table 3.2. shows the yield of cetyl palmitate over different metal salt hydrates. The experiments performed with different anionic parts such as chloride, nitrate, sulfate and acetate, and it was seen that there was no significant difference between the yields of esters. Thus, the activity of the catalysts were caused by the cationic metal moieties of the catalysts.

Table 3.2. The influence of type of metal salt on the yield of cetyl palmitate
(Source : Mantri et al.., 2007)

Metal	Yield of Cetyl Palmitate (%)			
	Chloride	Nitrate	Sulfate	Acetate
Fe^{3+}	95.8	93.5	88.2	
Al^{3+}	73.8	53.6	49.2	72.4
Ga^{3+}	97.5	98.0		
In^{3+}	98.6	95.6	89.1	
ZrO^{2+}	92.5	92.5	84.3	88.0
Zn^{2+}	81.5	76.6	79.5	78.2
Co^{2+}	70.5	71.8	72.2	29.8
Ni^{2+}	32.3	35.7	28.8	29.4
Cu^{2+}	37.7	38.2	32.0	29.8

Supporting these metal salt hydrates on ordered mesoporous silica enhanced the catalytic activity of the esterification although the activities depended on type of salt

hydrates. The reusability of the $FeCl_3 \cdot 6H_2O$ and $AlCl_3 \cdot 6H_2O$ supported on MCM-41 was examined and it was found that there was a significant decrease in the yield of cetyl palmitate for the $FeCl_3 \cdot 6H_2O$ catalysts due to the weak interactions between support and Fe ions. The results were better for $AlCl_3 \cdot 6H_2O$ catalysts with a decrease of 4% in the yield within 5 recycles of catalysts.

Sakthivel et al. (2008) studied the esterification of different fatty acids and fatty alcohols over MCM-48 supported tungstophosphoric acid under supercritical conditions (100 $^{\circ}$C , 11MPa CO_2 pressure). The amount of HPW loading was studied as a parameter, and it was found that the yield of esters increased until %20 loading and then decreased gradually with higher loadings. MCM-48 supported tungstophosphoric acid catalysts gave high yield of cetyl palmitate (% 96) at the first use of the catalyst. However, the yield decreased to % 37 at the end of the 4 th reuse of the catalyst, which indicated that the catalyst was not reusable. This was suggested to be due to leaching of the active heteropoly acid sites and inhibition of the catalyst with the water formed during the reaction.

From the literature, it can be concluded that the catalyst for the esterification reaction should have large surface area and high pore volume since the reactant molecules are large. Additionally the catalysts should have hydrophobic character because water is a side product of esterification reaction. Since esterification reaction is a reversible reaction and water can easily be adsorbed on the catalyst surfaces, the presence of water in the reaction mixtures is a disadvantage for the reaction. Another factor effecting the catalyst activity is the acidity of the catalyst. Especially the Bronsted acid sites are active sites for the reaction.

The studies of Mantri et al. (2005 and 2007) showed that zirconia was an effective active site for catalyst used in esterification reactions. It was also recyclable. Therefore, it can be mentioned as a green catalyst. The acidity of zirconia can be enhanced with loading of active sites such as tungsten oxide. Zirconia supported tungsten oxide catalyst has been studied in the literature for different reactions. Tungstated zirconia might be prepared by different methods such as impregnation, co-precipitation and sol-gel.

Vartuli et al. (1999) investigated the effects of the different preparation methods on the acidic properties of tungstated zirconia. Catalysts were prepared by co-precipitation, impregnation and co-precipitation containing iron. Co-precipitation method produced a greater number of acidic sites than impregnating tungsten on

hydrous zirconia, resulting in a more active catalyst. The addition of small amounts of iron to the tungsten/zirconia catalyst increased the acid site strength as determined by ammonia adsorption and improved the isomerization activity.The characterizations of the catalysts showed that the catalysts prepared by co-precipitation method had higher surface area than the catalysts prepared by impregnation. Also the stability of tetragonal zirconia phase which was the expected phase for high acidity increased by applying co-precipitation method instead of impregnation.

Santiesteban et al. (1997) investigated the influence of the preparative method on the activity of highly acidic WO_3-ZrO_2. They prepared tungstated zirconia by incipient wetness impregnation and co-precipitation. Also, they performed reflux prior to impregnation for the preparation of the catalysts. The results showed that, the acid side density of the tungstated zirconia prepared by co-precipitation was higher than the catalysts prepared by impregnation. The tetragonal phase of zirconia was required for high catalytic activity. The presence of tungsten oxide increased the stability of tetragonal zirconia phase. The catalyst had both Brønsted and Lewis acid sites.
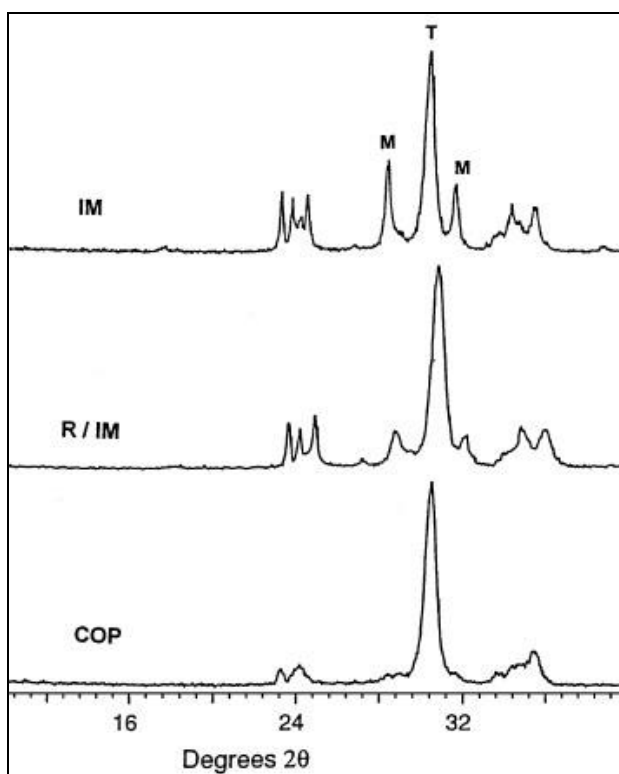

Figure 3.1 XRD spectra of catalysts prepared by different methods
(Source : Santiesteban et al., 1997)

Zhang et al. (2011) studied synthesis of acetyl salicylic acid over WO_3-ZrO_2 solid superacid catalyst. WO_3-ZrO_2 was prepared by co-precipitation of an aqueous zirconyl chloride and ammonium metatungstate solution. An aqueous zirconyl chloride

and ammonium metatungstate solution was heated to the boiling temperature, and was kept at reflux conditions for 2 h and then cooled. The results showed that, the loading of tungsten oxide in the catalyst inhibited the growth of monoclinic phase zirconia and stabilized the metastable tetragonal phase zirconia. The stabilization of the tetragonal zirconia phase with increasing WO_3 loading also effected the specific surface area of the catalysts. The surface area increased gradually with increasing WO_3 concentration up to 20 wt.%. The decrease in the surface area with further increase WO_3 concentration was related to the blockage of pores. Solid superacid WO_3-ZrO_2 was found to have excellent catalytic activity for synthesis of acetyl salicylic acid. WO_3-ZrO_2 solid superacids. The catalyst was easily recovered and reused repeatedly up to 4 reaction cycles with a consistent high yield.

As reported before, mesoporous silicas such as MCM-41 and SBA-15 were found as promising catalyst supports in the studies of (Mantri et al. (2005) and Mantri et al. (2007). These are two different types of mesoporous silica supports. Among these mesoporous silica materials SBA-15 was chosen for this study because of its hexagonal structure with a narrow pore size distribution and a tunable pore diameter between 5 and 15 nm. The thickness of the framework walls is about 3.1 to 6.4 nm, which gives the material a higher hydrothermal and mechanical stability than, for instance , MCM-41 (Thielemann et al. (2011)). Zirconia can be impregnated on the SBA-15 surface or it can be used in the synthesis of SBA-15 and so it can be integrated in the structure of SBA-15. There are examples of these kind of applications of Zr on mesoporous silicas in the litetature used in other reactions than esterification of long chain fatty acids and long chain fatty alcohols. Garg et al. (2009) studied SBA-15 containing various amount (10-50 wt%) of highly dispersed ZrO_2 prepared by urea hydrolysis method and this catalyst was used for esterification of cyclohexanol with acetic acid and cumene cracking. The results of this study showed that doping of zirconia inside SBA-15 did not destroy the hexagonal structure of SBA-15. As the ZrO_2 amount increased the total acidity and Bronsted acidity of catalysts increased whereas the Lewis acidity decreased. Both Lewis and Brønsted acidity passed through a max. at 35wt% ZrO_2 in SBA-15. The catalytic activity for both esterification and cracking reactions also passed a max. at around 35 wt% loading.

Morales et al. (2010) investigated the use of Zr doped MCM-41 supported WO_3 catalysts for the esterification of oleic acid with methanol. A series of zirconium doped MCM-41 silica supported WOx solid acid catalysts, with WO_3 loading ranging from 5

to 25 wt%, were prepared by impregnation with ammonium metatungstate, and subsequent activation at temperatures between 450 $^{\circ}$C and 800 $^{\circ}$C. The results showed that the interactions between (WO)x and superficial ZrO_2 on the pores of Zr-MCM-41 was very strong, especially at high activation temperatures and for high WO_3 loading. Due to this strong interaction WO_3/ Zr-MCM-41 catalysts were found reusable and stable for recycling.

Biswas et al. (2011) investigated the effect of different preparation methods to synthesize Zr-SBA-15 such as post synthesis (chemical grafting) and direct hydrothermal synthesis method. The characterizations of the resulting catalysts showed that Zr-SBA-15 had higher surface area when it was prepared by direct hydrothermal synthesis.

Hydrothermal synthesis method for Zr-SBA-15 was also investigated in the study of Gracia et al. (2009). Well structured Zr-SBA-15 mesoporous materials with high surface areas and narrow pore size distributions were obtained. Zr was confirmed by XPS and XRD to be incorporated within the framework of the SBA-15 materials. Zr-SBA-15 was found to have both Lewis and Brønsted acid sites.

Fuxiang et al. (2007) synthesized Zr-SBA-15 mesoporous materials with high Zr/Si ratio (0-2.32). Figure 3.2 shows the XRD patterns within the 2Θ range of 0.7 - 5 $^{\circ}$ of the Zr-SBA-15 samples. One very strong and two weak characteristic peaks of SBA-15 materials were clearly observed, which indicated that the hexagonal structure of SBA-15 was preserved throughout the synthesis and subsequent calcinations of Zr-SBA-15. With the Zr/Si molar ratio increasing during the synthesis process, the intensity of the peak near 2Θ = 0.9 decreased, and peaks indexed to 110 and 200 diffractions disappeared. This was considered to be due to gradually lowering of the long range order of the samples. However, the peak indexed to 100 was still observed when the Zr/Si ratio was 2.32. This indicated that the mesoporous structure was not destroyed until the Zr/Si molar ratio is over 2.62.
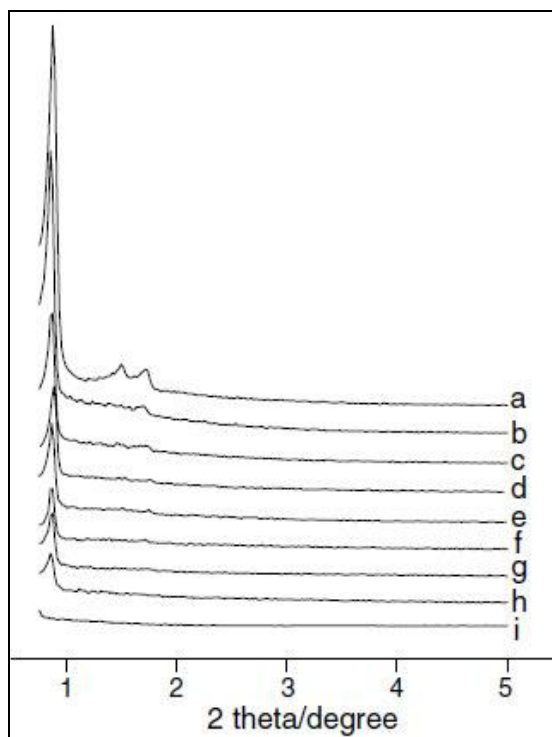
Figure 3.2. The XRD patterns of the samples Zr/Si: a-0, b-0.38, c-0.68, d-0.92, e-1.30, f-1.72, g-2.02, h-2.32, i-2.62

(Source: Fuxiang et al., 2007)

Zhang et al. (2009) studied Zr-SBA-15 supported WO_3 for the benzoylation of anisole. In this study they aimed to obtain a superacid catalyst with uniform mesoporous structure and high surface area. The Zr-SBA-15 supports were prepared by hydrothermal synthesis and the support was impregnated with various concentrations of ammonium metatungstate solutions (15 wt % - 35 wt%) and calcined at different temperatures (650 ^{o}C, 700 ^{o}C , 800 ^{o}C for 3 hours). The typical hexagonal structure was maintained for the sample loaded by WO_3 after calcination and showed a slight decrease in the order of hexagonal structured compared to the Zr-SBA-15. The XRD patterns of the catalysts having different WO_3 loading is given in Figure 3.3. The sample 15WZS973 showed no indication of any crystalline WO_3, which indicated uniform dispersion of WO_3 occured. This result suggested a strong interaction between WO_3 particles and the surface of Zr-SBA-15 after calcination.
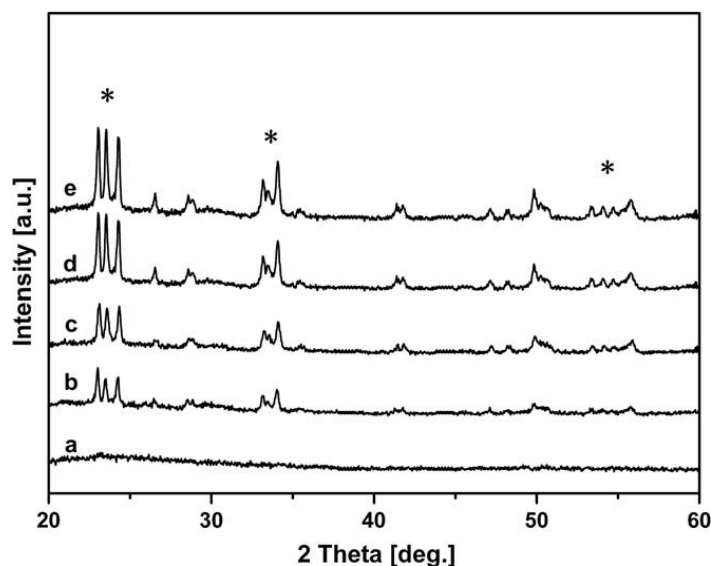
Figure 3.3. XRD patterns of WO$_3$/Zr-SBA-15 catalysts with different WO$_3$ loadings: a-15WZS973, b-20WZS973, c-25WZS973, d-30WZS973 and e-35WZS973 (Source : Zhang et al., 2011)

The catalysts showed both Lewis and Brønsted acid sites. Lewis acid sites were stronger than the Brønsted acid sites. In figure 3.4, the spectrum of Zr-SBA-15 the absorption bands at 1450, 1490 and 1609 cm^{-1} are indicative of presence of Lewis acid sites, while there was no Brønsted sites observed. On the other hand, all the spectra of the WO$_3$/Zr-SBA-15 samples exhibited bands assigned to pyridine coordinated on Lewis acid sites and Brønsted acid sites (1490 and 1540 cm^{-1}). The loading of WO$_3$ onto Zr-SBA-15 let to an increase of the number of Lewis acid sites.
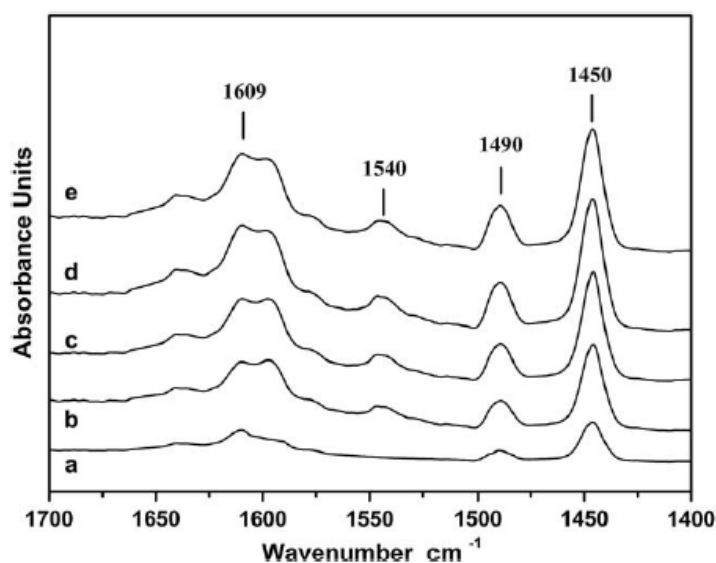
Figure 3.4. FTIR spectra of pyridine absorbed catalysts with different WO$_3$ loadings: a-Zr-SBA-15, b-20WZS923, c-20WZS973, d-20WZS1073, e-30WZS1073 (Source : Zhang et al., 2011)

In the light of the literature review given above, it was decided to synthesize co-precipitated WO$_3$-ZrO$_2$ catalysts and WO$_3$ loaded Zr incorporated SBA-15 catalysts for the esterification of cetyl alcohol and palmitic acid. The effect of WO$_3$ loading amount and calcination temperature was selected as experimental parameters. The reaction tests were performed with equimolar concentration of the reactants, and mesitylene was chosen as the solvent.

CHAPTER 4

EXPERIMENTAL STUDY

In this study it was aimed to develop heterogeneous catalysts for production cetyl palmitate by the esterification of cetyl alcohol and palmitic acid. For this purpose WO_3-ZrO_2, Zr incorporated SBA-15 and WO_3 loaded Zr-SBA-15 catalysts were synthesized and tested. Also WO_3-ZrO_2 catalysts were prepared by co-precipitation of an aqueous zirconyl chloride and ammonium metatungstate solution for comparison purposes. Synthesized WO_3-ZrO_2 catalysts with WO_3 wt% of 15% and 20% were labelled as WZ15 and WZ20 respectively. Zr incorporated SBA-15 catalyst was prepared via hydrothermal synthesis by using a gel with a molar composition of $0.017P123$:Si:$0.08Zr$:$220H_2O$, and labelled as Zr-SBA-15. Zr-SBA-15 was then used as support and impregnated with different loading amounts of WO_3 (15 wt% and 20 wt%) and calcined at different temperatures (700 ^{o}C and 800 ^{o}C)

4.1. Catalyst Preparation

4.1.1. Preparation of WO$_3$-ZrO$_2$ Catalysts

The chemicals used for the synthesis of WO_3-ZrO_2 is given in Table 4.1. WO_3-ZrO_2 was synthesized with two different WO_3 content as 15 wt% and 20 wt% and labelled as WZ15 and WZ20 respectively.

Table 4.1. The chemicals used for the synthesis of WZ15 and WZ20

Chemicals	
Ammonium metatungstate hydrate	Aldrich $\geq$ 85 % WO_3 basis
Zirconium(IV) oxychloride octahydrate	Sigma aldrich $\geq$ 99.5 %
Ammonium hydroxide solution	Riedel de Haen 26%

For the synthesis of WZ15 two solutions were prepared. Solution A: 0.75 g of ammonium metatungstate hydrate was dissolved in 6 ml of deionized water at room

temperature. Solution B: 8.94 g of zirconium(IV) oxychloride octahydrate was dissolved in 125.45 ml of deionized water at room temperature. These two solutions were mixed in a 200 ml round bottom flask equipped with a reflux condenser and magnetic stirrer. The mixture was heated to the boiling temperature and kept at reflux conditions for 2 h and then cooled. The pH of the resulting solution was adjusted to 9.5 by adding ammonium hydroxide solution dropwise with magnetic agitation. A jelly precipitate was formed, then was aged for 24 h at ambient conditions. The aged precipitate was centrifuged and washed with excess amount of deionized water to remove the chlorides. After that, the collected solid was dried at 110 ^{o}C overnight, and calcined in air at 700 ^{o}C for 3 h.

The same procedure was followed for the preparation of WZ20. Here 1 g of ammonium metatungstate hydrate dissolved in 8 ml of deionized water was added to a solution which contained 8.25 g of zirconium(IV) oxychloride octahydrate in 116.36 ml of deionized water at room temperature.

4.1.2. Preparation of Zr-SBA-15 Catalyst

The chemicals used for the synthesis of Zr-SBA-15 is given in Table 4.2.

Table 4.2. The chemicals used for the synthesis of Zr-SBA-15

Chemicals	
Pluronic P123	Aldrich average M_n ~5,800
Zirconium(IV) oxychloride octahydrate	Sigma aldrich $\geq$ 99.5 %
Tetraethyl orthosilicate (TEOS)	Aldrich 98%

Firstly, 5 g of the amphiphilic triblock copolymer P123 (EO20PO70EO20) used as the structure-directing agent was dissolved in 150 ml of deionized water at 37 ^{o}C with continuously stirring until obtaining a clear micelle solution. Secondly, 1.311 g of zirconium(IV) oxychloride octahydrate was dissolved in 50 ml deionized water at room temperature. Thirdly, 11.53 ml of TEOS and the aqueous zirconium(IV) oxychloride octahydrate (ZrOCl$_2$.8H$_2$O) solution was added into the P123 solution. Fourthly, the mixture was vigorously stirred at 37 ^{o}C for 24 h. Afterwards the gel formed, with a molar composition of 0.017P123:Si:0.08Zr:220H2O was transferred into a Teflon-lined stainless steel autoclave. The autoclave was then sealed and kept at 90 ^{o}C for 24 h. The

product obtained was centrifuged with a large amount of deionized water to remove the weakly adsorbed ions. This was followed by drying overnight at ambient conditions. Finally it was calcined at 800 ^{o}C for 4 h. The heating rate to 800 ^{o}C was 2 ^{o}C/ min.

4.1.3. Preparation of WO$_3$/Zr-SBA-15 Catalysts

WO$_3$ was loaded onto Zr-SBA-15 catalyst by incipient wetness impregnation. Two different loadings were performed; 15 wt % and 20 wt% . For 15 wt% WO$_3$ loading, 1 g of Zr-SBA-15 was added to 0.188 g of ammonium metatungstate hydrate dissolved in 4 ml of deionized water. The mixture was kept in an ultrasonic bath to improve WO$_3$ dispersion. After filtration and drying in an oven at 110 ^{o}C for 12 h, it was heated to calcination temperature with a heating rate of 2 ^{o}C/ min.. Two different calcination temperatures, 700 ^{o}C and 800 ^{o}C were employed for 3 h.

Similar procedure was followed for preparation 20 wt% WO$_3$. Here, 0.251 g of ammonium metatungstate hydrate dissolved in 4 ml of deionized water was added to 1 g of Zr-SBA-15 was impregnated with this solution. The catalysts prepared are named as given in Table 4.3.

Table 4.3. The labels of prepared WO$_3$/Zr-SBA-15 catalysts

Catalyst	Catalyst Specifics
WZSBA15-15-7	15 wt % WO$_3$ loading, 700 ^{o}C calcination
WZSBA15-15-8	15 wt % WO$_3$ loading, 800 ^{o}C calcination
WZSBA15-20-7	20 wt % WO$_3$ loading, 700 ^{o}C calcination
WZSBA15-20-8	20 wt % WO$_3$ loading, 800 ^{o}C calcination

4.2. Characterization of Catalysts

4.2.1. BET

Nitrogen physisorption studies were performed using Micromeritics ASAP 2010 model static volumetric adsorption instrument. WZ15 and WZ20 catalysts were degassed at 200 ^{o}C for 4 hours prior to adsorption experiments, whereas other catalysts

(Zr-SBA-15, WZSBA15-15-7, WZSBA15-15-8, WZSBA15-20-7 and WZSBA15-20-8) were degassed at 200 ^{o}C for 2 hours. N_2 adsorption was performed at 77 K.

4.2.2. X-Ray Diffraction

The crystalline structures of the catalysts were determined by Philips X'Pert diffractometer with CuKα radiation. The scattering angle 2θ was varied from 5 °C to 80 °C, with a step length of 0.02.

4.2.3. Low Angle X-Ray Diffraction

Low angle XRD analysis of the Zr-SBA-15 and WO_3 / Zr-SBA-15 catalysts was performed at METU Central Laboratory on Rigaku Ultima IV X-Ray Diffractometer using CuKα radiation (λ=0,154 nm). The 2θ value was scanned in the range of $0.5 - 80^o$ with a resolution of 2 min^{-1}.

4.2.4. Raman Spectroscopy

Raman spectra for WZ15 and WZ20 catalysts were obtained by an Argon laser at the excitation wavelength of 514 nm. The resolution was 4 cm^{-1} , 2 cm^{-1} and 1 cm^{-1}.

4.2.5. Skeletal FTIR Spectroscopy

The framework vibration of synthesized Zr-SBA-15 and WO_3/Zr-SBA-15 catalysts was examined by FTIR spectroscopy. KBr pellet technique was employed to obtain infrared spectra of the samples at room temperature. The pellets were prepared with a sample amount of 3 wt%. The spectra were retrieved in the wavenumber range of 400 - 2000 cm^{-1} with a resolution of 4 cm^{-1} by an infrared spectrometer type Schimadzu FTIR 8400S.

4.2.6. Temperature Programmed Desorption of Ammonia

The acidity of the catalysts was determined by Temperature-Programmed Desorption of Ammonia (NH_3-TPD) method using Micromeritics AutoChem II Chemisorption Analyzer instrument.

The catalyst samples were heated up to 400 °C by increasing the temperature at a rate of 5 °C/min and kept at this temperature for 30 minutes under He gas flow of 70 ml/min. Then the sample was cooled under He flow of 30 ml/min to 60 °C at a rate of 5 °C/min. This was followed by switching the flow to NH_3-He gas mixture at the rate of 30 ml/min for 30 min. Physically adsorbed NH_3 was removed by degassing the sample at 60 °C under He flow of 70 ml/min for 120. NH_3 desorption of the sample was analyzed by heating the sample at the rate of 10 °C/min from 60 °C to 700 °C. TCD signal was recorded during the NH_3-TPD.

4.2.7. Pyridine Adsorbed FTIR

Brønsted and Lewis acidity characteristics of the catalysts were determined by IR spectroscopy using pyridine adsorption/desorption method. For the analysis, the samples were activated at 300 °C under vacuum (2×10^{-2} mmHg) for 2 h. Adsorption of pyridine was carried out at 150 ºC for 30 minutes. Before FTIR analysis the samples were kept 120 °C under N_2 flow of 30 ml/min for 2 h in order to desorb the physisorbed pyridine.

IR analysis were carried out between 400 and 4000 cm^{-1} with Shimadzu FTIR 8400S model Fourier Transformed Infrared Spectrometer using KBr pellet technique. KBr pellets were prepared by pressing a mixture of 4.5 mg of pyridine adsorbed catalyst sample and 150 mg KBr.

4.2.8. XRF Analysis

Elemental composition of the catalyst that gave the highest conversion was analyzed by XRF method before and after its use in the reaction. The analysis was performed with powder method by using Spectro IQ II instrument and CuKα radiation.

4.3. Catalyst Testing

In reaction tests, palmitic acid (Sigma P0500) and cetyl alcohol (Fluka 52238) were the reactants and mesitylene (Aldrich 140864) was the solvent. The tests were performed in a four necked round bottom flask (250 ml) equipped with a Teflon coated magnetic stirring bar and a Dean Stark apparatus surmounted with a reflux condenser. The reactions were performed at 162 ^{o}C under N_2 atmosphere with a N_2 flow of 35 ml /min. The reaction set-up is shown in Figure 4.1.

Figure 4.1. The reactor set-up

The progress of the reaction was followed by taking samples (0,5 ml) from the reaction mixture at specified time intervals (0, 30, 60, 120, 180, 240 and 360 min). After cooling the samples in the fridge, they were centrifuged (13000 rpm for 3,5 minutes) to remove catalysts. The samples were then diluted 10 times with dichloromethane for analysis.

The products were analysed by Agilent 6890 gas chromatograph using Ultra 1 (25 m x 0,3 mm) capillary column equipped with FID. The injector temperature was 280 ^{o}C and the detector temperature was 320 ^{o}C. The GC oven temperature was programmed from 50°C at 12 ° C/ min to 300°C where it was kept for 35 min. Helium was used as the carrier gas at a flow rate of 37,3 mL / min; the split ratio was 24,9:1.

For quantification of the products, calibration curves of palmitic acid, cetyl alcohol and cetyl palmitate were obtained by using mixed standard of these chemicals.

4.3.1. Esterification of Cetyl Alcohol and Palmitic Acid with Homogeneous Catalyst

The first reaction tests were performed with homogenous catalyst using $ZrOCl_2.8H_2O$. For a standard reaction test, 40 mg of $ZrOCl_2.8H_2O$ was added into 25 ml of mesitylene and heated up to 162 ^{o}C under N_2 atmosphere. An equimolar solution of palmitic acid and cetyl alcohol containing 6 mmole of palmitic acid and cetyl alcohol in 15 ml of mesitylene (0,4 M) at room temperature was added into the reactor. After that the samples (0,5 ml) were taken for different reaction time into a GC vials. The samples were kept in the fridge until the product analysis.

In addition excess moles of cetyl alcohol was also tested in the reaction in order to see the equilibrium effect on the reaction by using 18 mmoles of cetyl alcohol (0.45 M) and 6 mmoles of palmitic acid (0.15 M) under the same conditions.

4.3.2. Esterification of Cetyl Alcohol and Palmitic Acid Over Heterogeneous Catalysts

The first reaction tests over heterogeneous catalysts were performed by using WZ15 and WZ20 catalysts. 40 mg of catalyst was added into 25 ml of mesitylene and heated up to 162 ^{o}C under N_2 atmosphere. Reaction conditions and the amount of reactants was the same as the reactions with the homogeneous catalyst. The effect of catalyst amount was also investigated by increasing the amount of WZ20 catalyst from 40 mg to 80 mg.

WZSBA15-15-7 and WZSBA15-20-7 catalysts were tested in the reaction under the same reaction conditions. The different amounts of these catalysts 40 mg, 80 mg and 160 mg were investigated. As higher conversions were obtained with 160 mg catalyst, this amount was considered in further tests of WZSBA15-15-8, WZSBA15-20-8, and Zr-SBA-15 catalysts.

The effect of the reactant composition was tested over the catalysts that gave the highest conversion by using the reactants with a cetyl alcohol : palmitic acid mole ratio of 3:1.

CHAPTER 5

RESULTS AND DISCUSSION

5.1. Characterization of the Catalysts

5.1.1. WZ15 and WZ20 Catalysts

The crystal structure of WZ15 and WZ20 catalysts (WO_3-ZrO_2 prepared by co-precipitation with 15 wt% and 20 wt% WO_3) was investigated with X-Ray Difraction. Figure 5.1 shows the XRD pattern of the catalysts. The XRD patterns of these two catalysts showed that the only existing phase of zirconia was the tetragonal phase as expected. The addition of WO_3 stabilized the metastable tetragonal phase of zirconia. There was no WO_3 crystalline phase observed in XRD spectra indicating the monolayer dispersion of tungsten species.
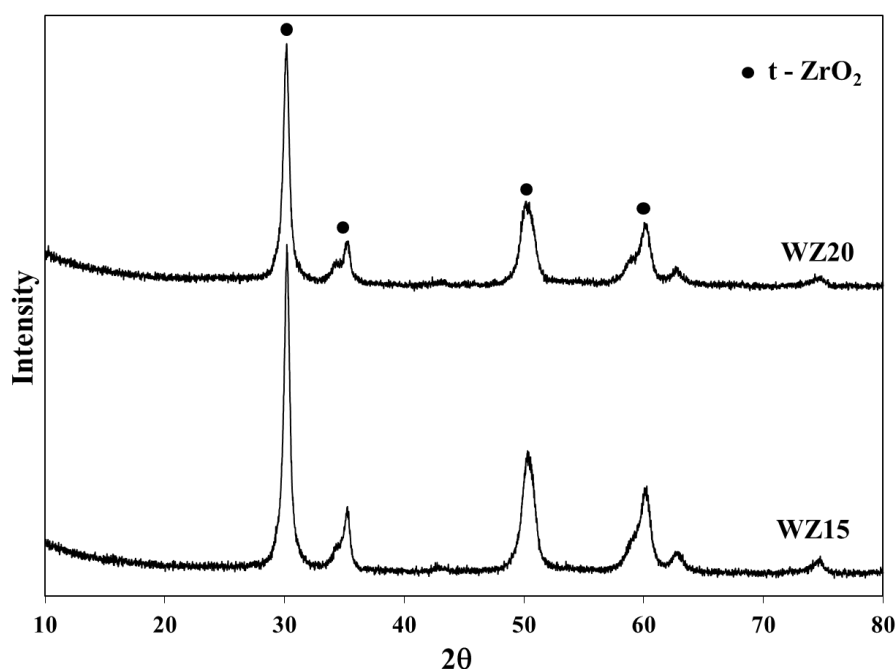
Figure 5.1. XRD patterns of WZ15 and WZ20 catalysts

The results of Raman spectroscopy were consistent with the results of XRD analysis. Figure 5.2 shows the Raman spectra for WZ15 and WZ20. The presence of peaks at 323 cm^{-1} and 640 cm^{-1} indicated the metastable tetragonal zirconia phase. By comparing the spectra, it can be observed that as the amount of WO$_3$ increased the intensities of tetragonal ZrO$_2$ peaks increased. Additionally, the band observed at 993 cm^{-1} indicated the monolayer WO$_3$.
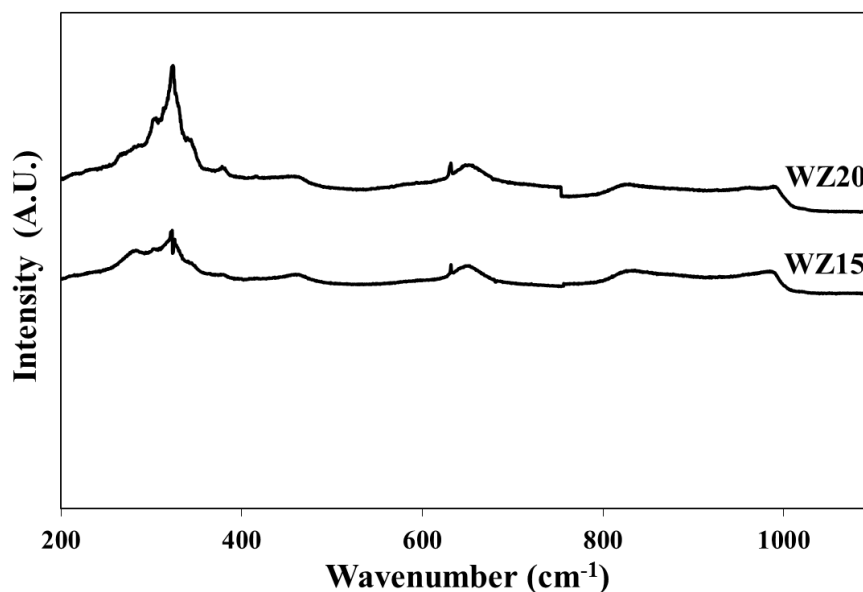

Figure 5.2. Raman spectra of WZ15 and WZ20 catalysts

The specific surface area, cumulative pore volume and pore diameter of WZ15 and WZ20 determined by N$_2$ adsorption. WZ15 and WZ20 catalysts showed type-IV adsorption isotherms with a hysteresis loop as given in Figure 5.3. The extent of the hysteresis decreased with WO$_3$ concentration. The specific surface area, pore diameters and pore volumes were given in Table 5.1. The pore diameter of catalysts were 31 Å. The specific surface area increased with increasing WO$_3$ concentration from 15 to 20 wt.%. This confirmed the surface area stabilizing effect of tungsten oxide on ZrO$_2$. It is likely that the interaction between tungsten oxide and ZrO$_2$ inhibits sintering and delays crystal growth, favoring the stabilization of the tetragonal zirconia as indicated from XRD pattern. This results are consistent with the results of the study by Zhang et al. (2011).
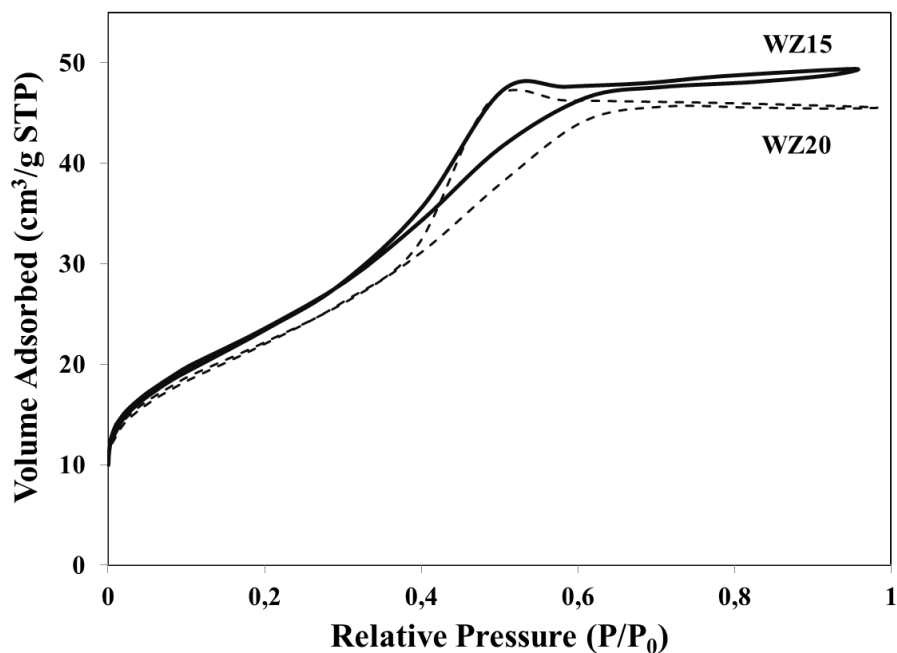
Figure 5.3. N_2 adsorption isotherms of the WZ15 and WZ20 catalysts

Table 5.1. Textural properties and acidities of WZ15 and WZ20

	Pore Diameter (Å)	Pore Volume (cm³/g)	BET Surface Area (m²/g)	External Surface Area (m²/g)	Total Acidity (mmol NH₃/g cat)
WZ15	31.9	0.061	81.3	79.9	0.26
WZ20	31.3	0.066	87.8	87.5	0.19

The acidity of WZ15 and WZ20 was determined by NH_3-TPD. The results are shown in Figure 5.4. The desorption peaks are centered at low temperature (150 ^{o}C) and high temperature (350 ^{o}C) are referred to as weak and strong acid sites respectively. the TPD profiles showed that for both of the catalysts, the acid strength was broadly distributed over the temperature range. The acidity of the catalysts were determined by using the area under the TPD profiles. The resulting total acidity values are given in Table 5.1. WZ15 had higher acidity than WZ20.
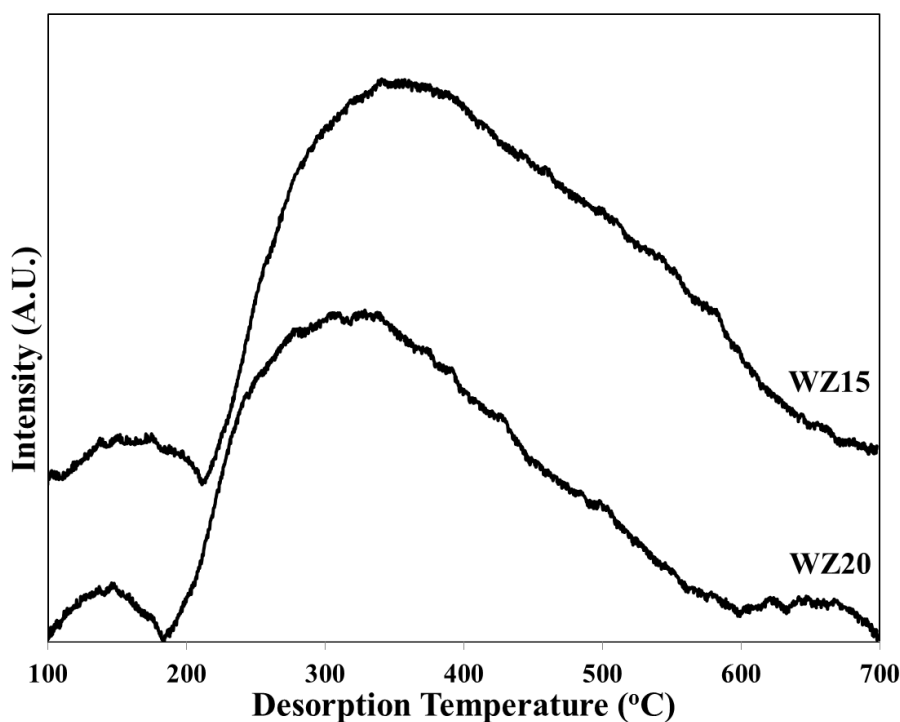
Figure 5.4. NH$_3$-TPD profiles of WZ15 and WZ20

5.1.2. Zr-SBA-15 and WZSBA15 Catalysts

The powder XRD patterns at low angles from 1 ^{o}C to 5 ^{o}C of the Zr-SBA-15 and WZSBA15 (WO$_3$ loaded Zr incorporated SBA-15) catalysts are shown in Figure 5.5. Zr-SBA-15 exhibited three distinct diffraction peaks corresponding to the reflections at (100), (110) and (200). These are the characteristic of 2D hexagonal structure of SBA-15. Therefore it could be concluded that the hexagonal structure of SBA-15 was preserved after Zr incorporation. When the spectra of tungsten loaded samples were examined, it was observed that the intensities of the characteristic peaks decreased with loading of tungsten. This might be caused by the decrease in the orderliness because of the introduction of WO$_3$ into the mesoporous channels of Zr-SBA-15.
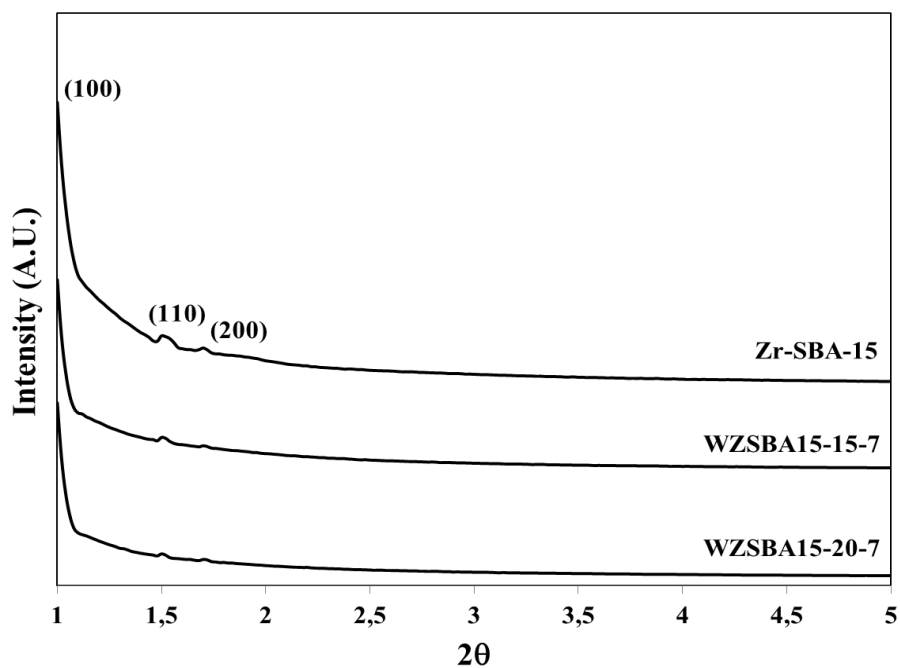
Figure 5.5. XRD patterns of Zr-SBA-15 and WO$_3$/Zr-SBA-15 catalysts at low angle

Skeletal FTIR spectra of Zr-SBA-15 was given in Figure 5.6. The band observed at the interval of 1070 cm^{-1} and 1220 cm^{-1} was caused by symmetric stretching of Si-O-Si bonds. The peak at 465 cm^{-1} was caused by the vibration of Si-O-Si bond. Except from these peak and band, a band was observed at 966 cm^{-1} which was caused by the vibration of Si-O-Zr bond. The existence of this band showed the success of Zr incorporation.
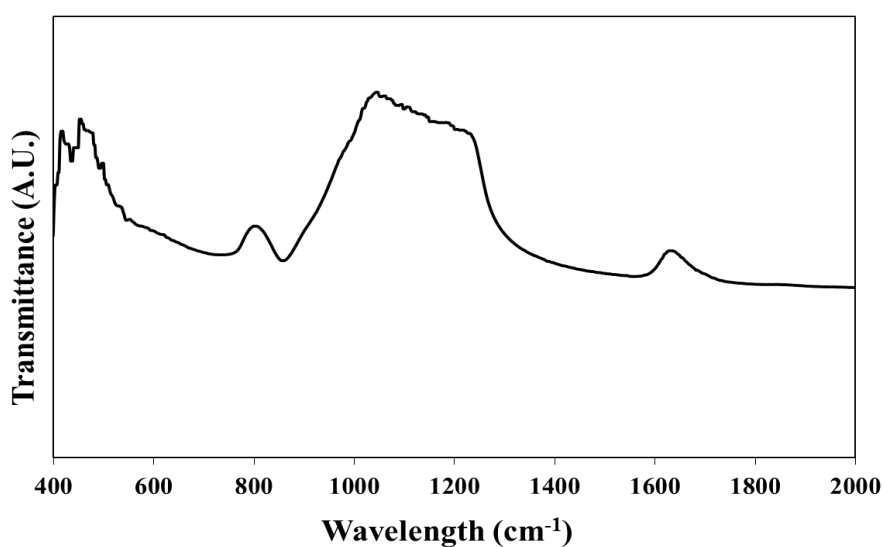
Figure 5.6. Skeletal FTIR spectra of Zr-SBA-15

Figure 5.7 displays the XRD patterns of WZSBA15 catalysts at higher angles from 20 ^{o}C to 60 ^{o}C. The labelled diffraction peaks are related to WO_3 crystals. The intensities of these peaks increases with increasing the loading amount and decreasing the calcination temperature of the catalysts. The results provided the evidence that after thermal treatment the WO_3 crystals transform into smaller tungsten oxide particles and change into well dispersed species on the Zr-SBA-15 surface. These results are in good agreement with the literature (Zhang et al., 2009).
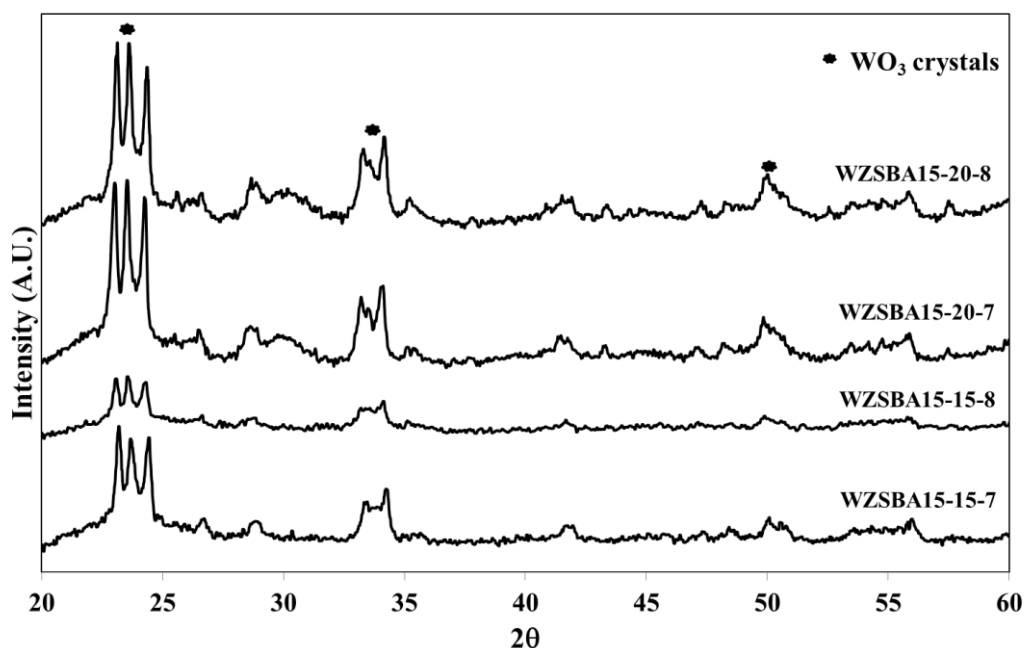
Figure 5.7. XRD patterns of WO_3/Zr-SBA-15 catalysts

The N_2 adsorption isotherms of SBA-15 based catalysts are given in Figure 5.8. The catalysts exhibited a type-IV isotherm with a hysteresis loop, which correspond to a hexagonal pore system. It was clearly observed from Figure 5.8, that the height of the hysteresis loop decreased with loading of WO_3. The results are consistent with the results of the studies in the literature (Biswas et al. (2011), Zhang et al., (2009)). The specific surface area, pore diameters and pore volumes of the catalysts are given in Table 5.2. The surface area of Zr-SBA-15 was 600.3 m^2/g which was decreased significantly, almost upto 50 %, with WO_3 loading. The higher loading decreased the surface area more. Also increasing calcination temperature decreased surface area. Accordingly, pore sizes were dropped by loading and calcination. The pore diameters of the catalysts were found in the interval of 37.3 Å and 45.5 Å.
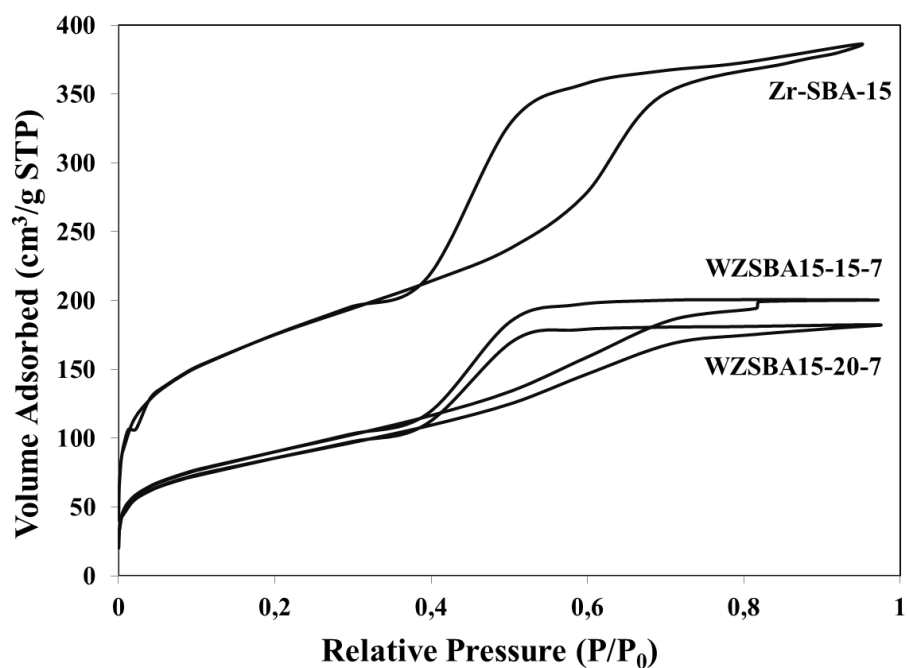
Figure 5.8. N$_2$ adsorption isotherms of the catalysts

Table 5.2. Textural properties and acidities of the catalysts

	Pore Diameter (Å)	Pore Volume (cm^3/g)	BET Surface Area (m^2/g)	External Surface Area (m^2/g)	Total Acidity (mmol NH$_3$/g cat)
Zr-SBA-15	42.4	0.4	600.3	530.2	0.152
WZSBA15-15-7	37.6	0.2	318.7	294.2	0.102
WZSBA15-15-8	25.9	0.1	230.0	213.8	0.202
WZSBA15-20-7	37.3	0.2	299.8	274.7	0.099
WZSBA15-20-8	25.1	0.1	180.4	172.9	0.159

Table 5.3 displays the results of elemental analysis of Zr-SBA-15 before and after the reaction. There was no significant decrease in the content of Zr after the reaction.

Table 5.3. Elemental analysis of fresh and used Zr-SBA-15

	Zr %	ZrO$_2$%
Fresh	5.99	8.06
Used Catalyst	5.82	7.87

Acidity of the catalysts determined by ammonia TPD are given in Figure 5.9. The total acidity of the catalysts obtained from this figure are given in Table 5.2. The

catalysts were found to have different total acidity and their acid sites changed depending on the catalyst. WZSBA15-15-8 had much acidity than other catalysts. This was followed by Zr-SBA-15. The catalysts acidity improved by higher calcination temperature. This might be explained by the effect of presence of WO_3 crystals.
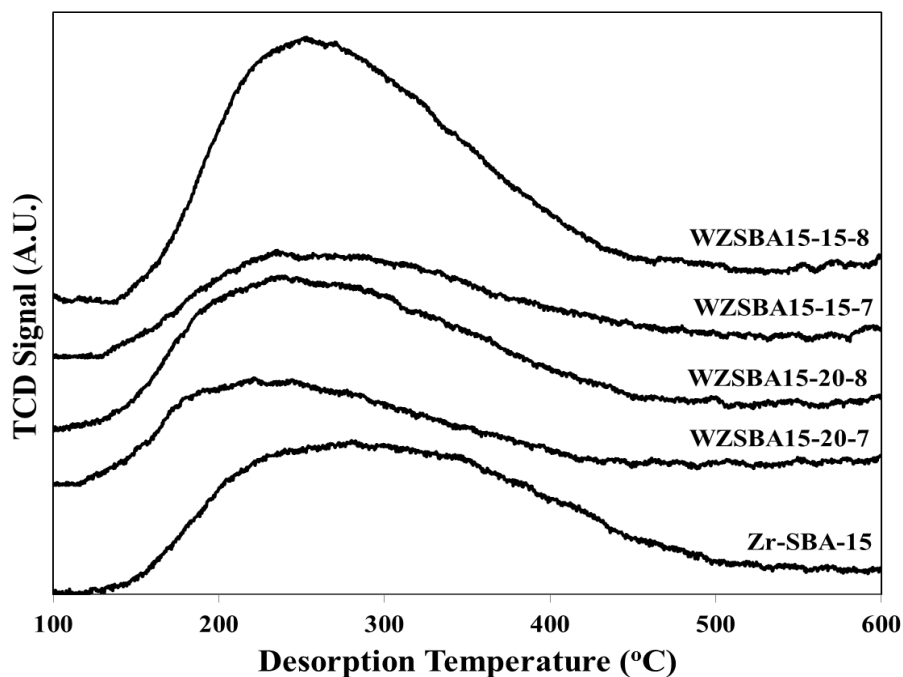

Figure 5.9. NH_3-TPD profiles of Zr-SBA-15 and WO_3/Zr-SBA-15 catalysts

Figure 5.10 shows the acid types of Zr-SBA-15 and WZSBA-15 based catalysts. For all catalysts peaks were observed at 1445 cm^{-1} , 1495 cm^{-1} and 1540 cm^{-1}. The peak at 1445 cm^{-1} indicates the Lewis acid sites , 1495 cm^{-1} indicates both the Lewis and Brønsted acid sites and 1540 cm^{-1} indicates Brønsted acid sites. The higher the peak area, the more acid amount is. When the area of the peaks were compared, the highest peak was observed for Zr-SBA-15. When the spectra of WZSBA15-15-7 and WZSBA15-20-7 were compared, it was observed that as the loading amount increased, the intensities of the peaks at 1445 cm^{-1} and 1495 cm^{-1} decreased clearly. This implied that acidity of the catalysts decreased with WO_3 loading. This might be caused by the WO_3 crystals existing on WZSBA15-20-7 catalyst. The XRD spectra in Figure 5.7 showed that the amount of WO_3 crystals increased with increasing calcination temperature. Correspondingly, the intensities of the peaks observed in FTIR spectra increased with calcination temperature. The results are also consistent with the results of NH_3-TPD.
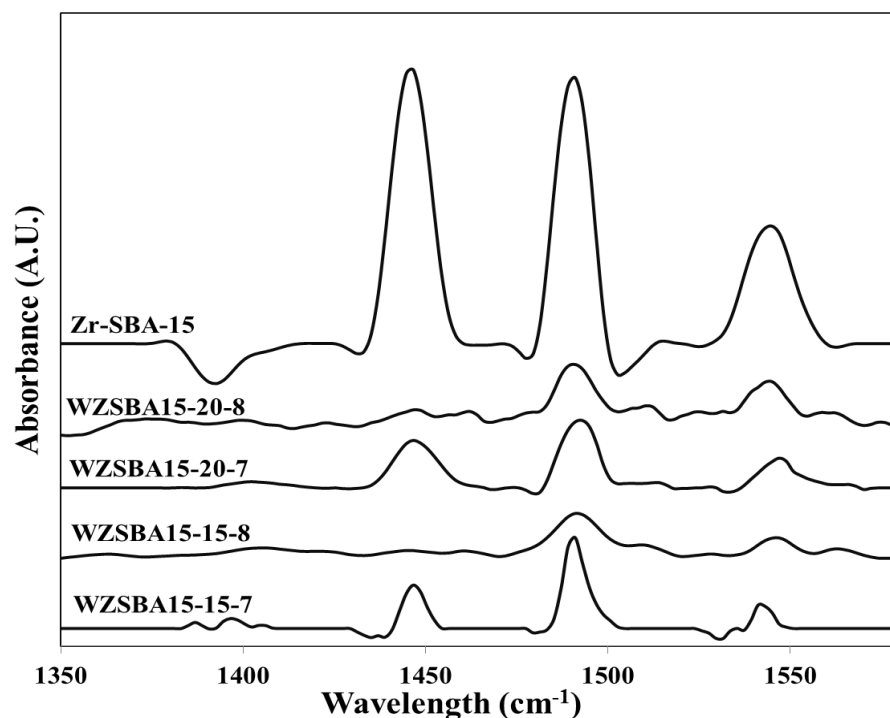
Figure 5.10. FTIR spectra of pyridine adsorbed Zr-SBA-15 and WO$_3$/Zr-SBA-15 catalysts

5.2. Catalyst Testing

The reaction tests were performed both with homogeneous and heterogeneous catalysts under the same reaction conditions. The effect of the amount of the catalysts and the reactant composition were investigated as reaction parameters.

The conversion of cetyl alcohol (CA), yield of cetyl palmitate (CP) and the selectivity to CP was calculated as given below.

$$Conversion(\%) = \frac{(CA_{in} - CA_{out})}{CA_{in}} x100$$

$$Yield\,(\%) = \frac{CP_{out}}{CA_{in}} x100$$

$$Selectivity\;\;to\;\;CP(\%) = \frac{CP_{out}}{(CA_{in} - CA_{out})} x100$$

5.2.1. The Reaction Tests With Homogeneous Catalyst

The first reaction tests were performed with $ZrOCl_2.8H_2O$. In order to observe the effect of equilibrium conditions both equimolar and excess reactant ratios were tested. For the test of excess reactant three times more cetyl alcohol was used in the reaction. The concentration of reactants and product are given in Figure 5.11 and Figure 5.12. Cetyl palmitate was the sole product. The concentration of reactants dropped slowly and so that of products increased slowly.
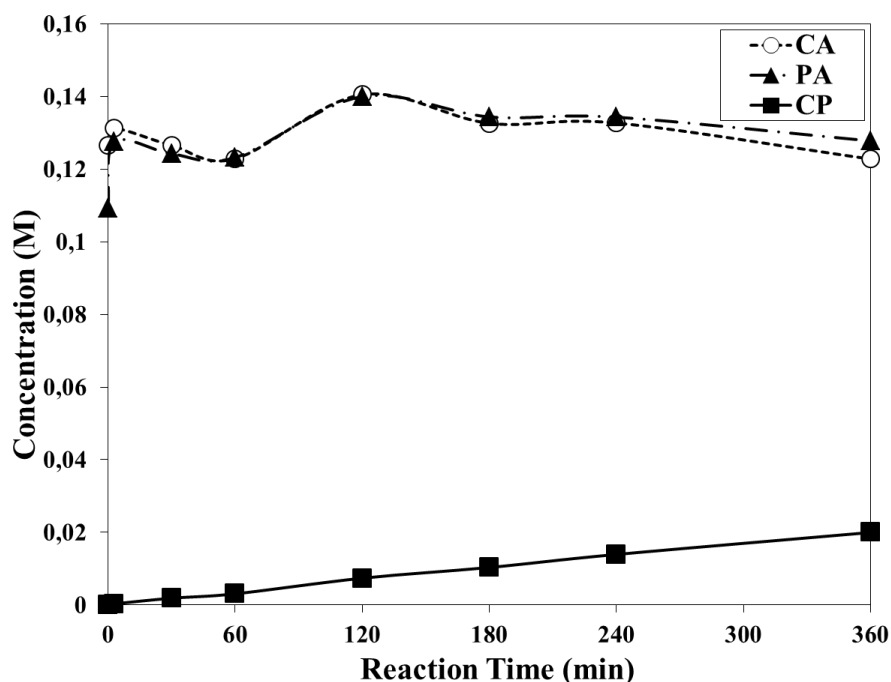
Figure 5.11. The change in concentration reactants and product with time (CA:PA mole ratio = 1:1)

To assess the effect of equilibrium on the reaction, the reaction was performed for cetyl alcohol/palmitic acid ratio of 3. The result obtained is given in Figure 5.12. A similar concentration change of species was observed with cetly alcohol/palmitic acid ratio of 1. Cetyl alcohol conversions obtained both for equimolar and excess cetyl alcohol (cetyl alcohol/palimitic acid ratio of 1/3) are given in Figure 5.13. The results showed that cetyl alcohol conversion was not affected significantly by excess cetyl alcohol. Therefore it could be deduced tthat the reaction was not limited by equilibrium constraints under the conditions studied.
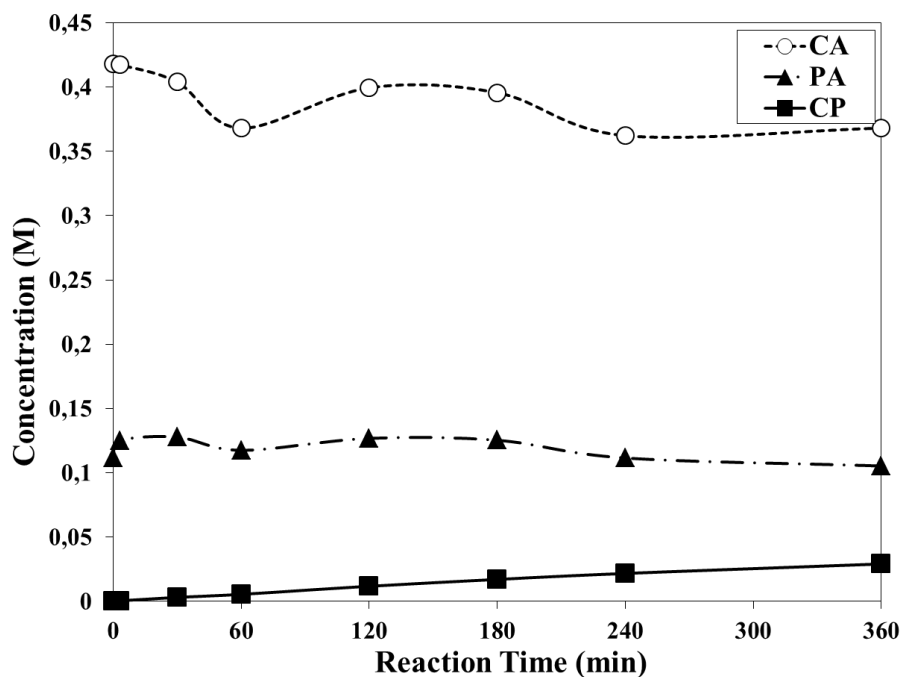
Figure 5.12. The change in concentration reactants and product with time (CA:PA mole ratio = 3:1)
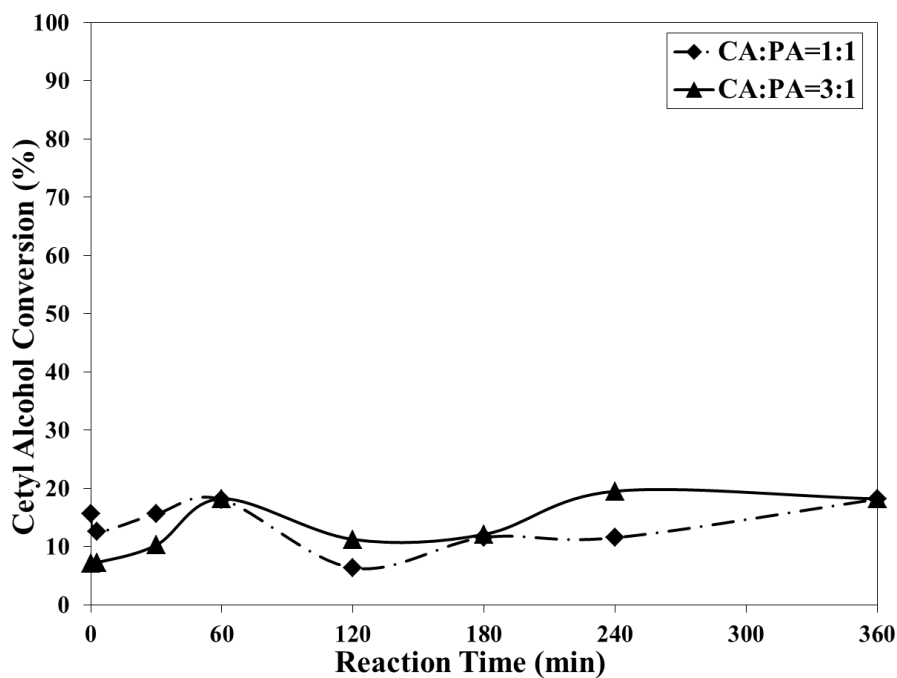

Figure 5.13. Conversion of cetyl alcohol with homogeneous catalyst ($ZrOCl_2.8H_2O$)

5.2.2. The Reaction Tests With Heterogeneous Catalysts

First reaction tests with heterogeneous catalysts were performed over WZ15 and WZ20. The catalyst amount was 40 mg. The concentration change with respect to time

are given in Figures 5.14 and 5.15. The concentration of cetyl alcohol decreased slowly with reaction time. Cetyl palmitate was the only product.
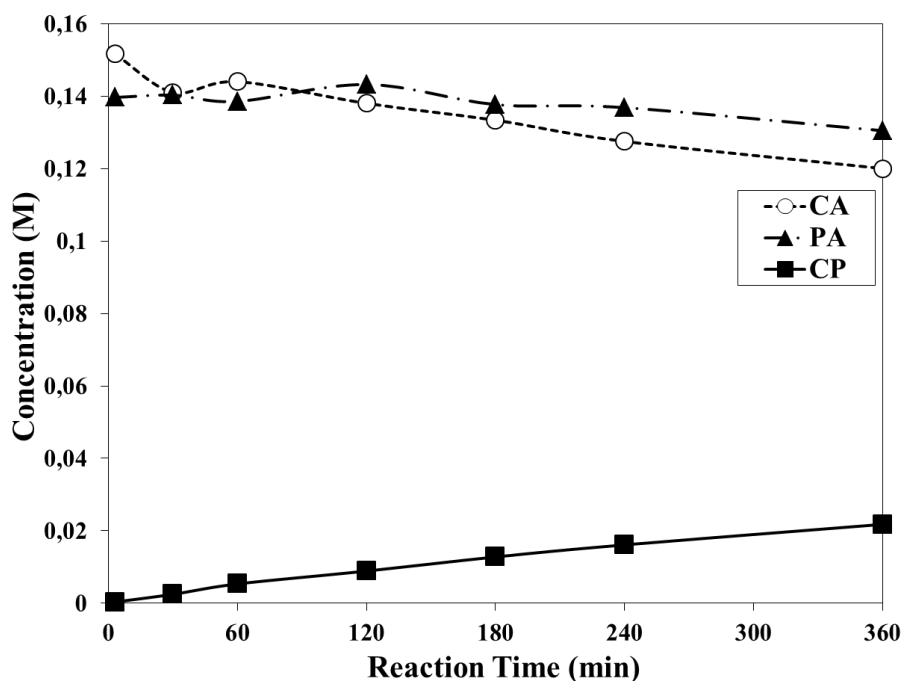
Figure 5.14. The change in concentration reactants and product with time over 40 mg of WZ15
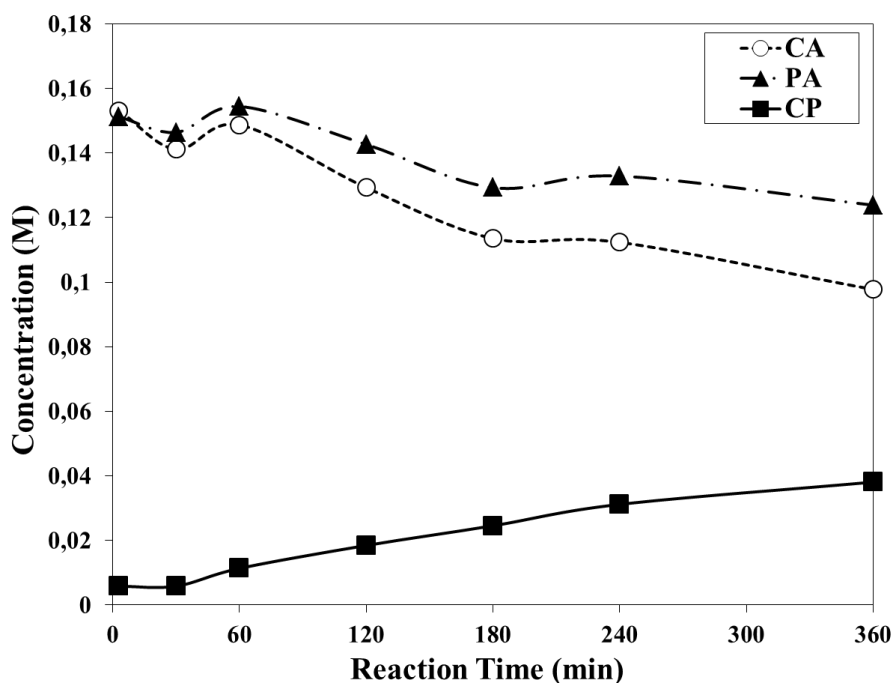
Figure 5.15. The change in concentration reactants and product with time over 40 mg of WZ20

Figure 5.16 displays the conversion change with time over the catalysts. The conversion of cetyl alcohol over WZ20 (35%) was higher than that over WZ15 (25%). WZ20 which gave the higher conversion was tested by increasing the amount twice in order to determine the effect of catalyst amount on the conversion. It was seen that the conversion over WZ20 increased to 70 % from 35 % when the amount of the catalyst increased. It showed that the reaction is kinetically controlled.
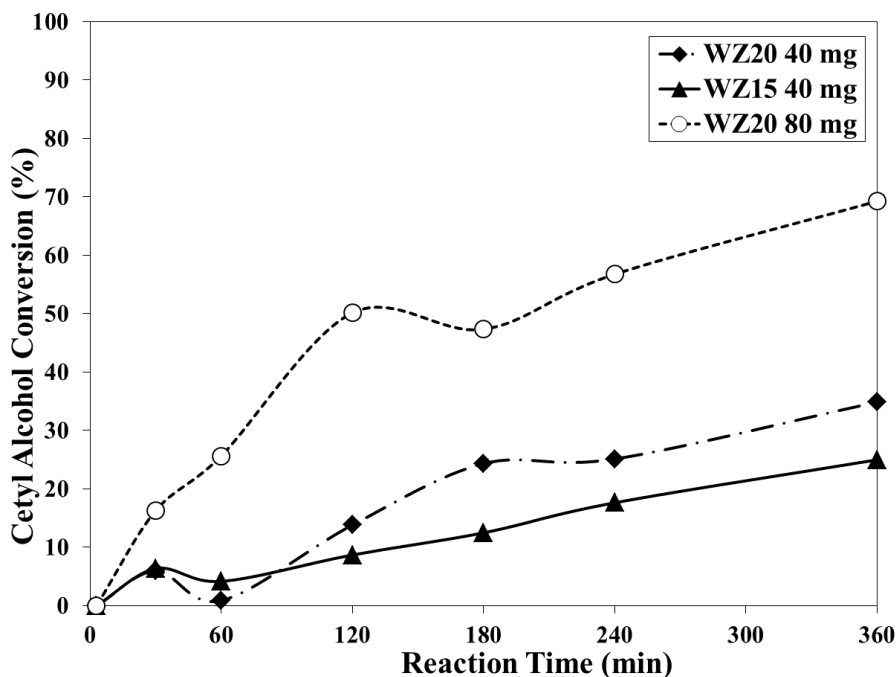

Figure 5.16. Conversion of cetyl alcohol over WZ15 and WZ20

The reaction tests were continued with testing the effect of catalyst amount for WZSBA15-15-7 The concentration changes of reactants and product are given in Figures 5.17, 5.18 and 5.19. The cetyl palmitate was the only product.
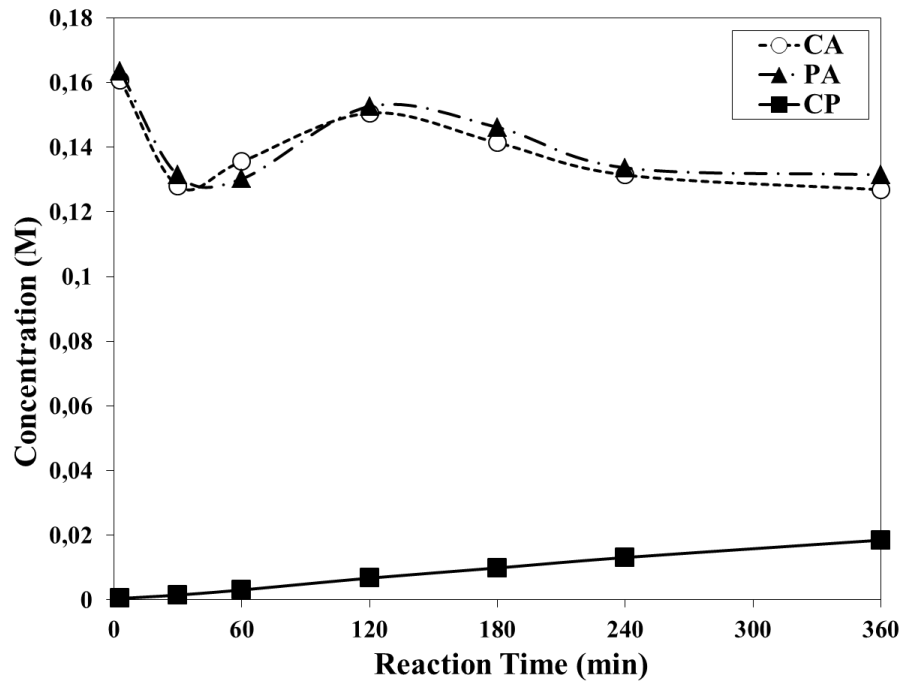
Figure 5.17. The change in concentration reactants and product with time over 40 mg of WZSBA15-15-7
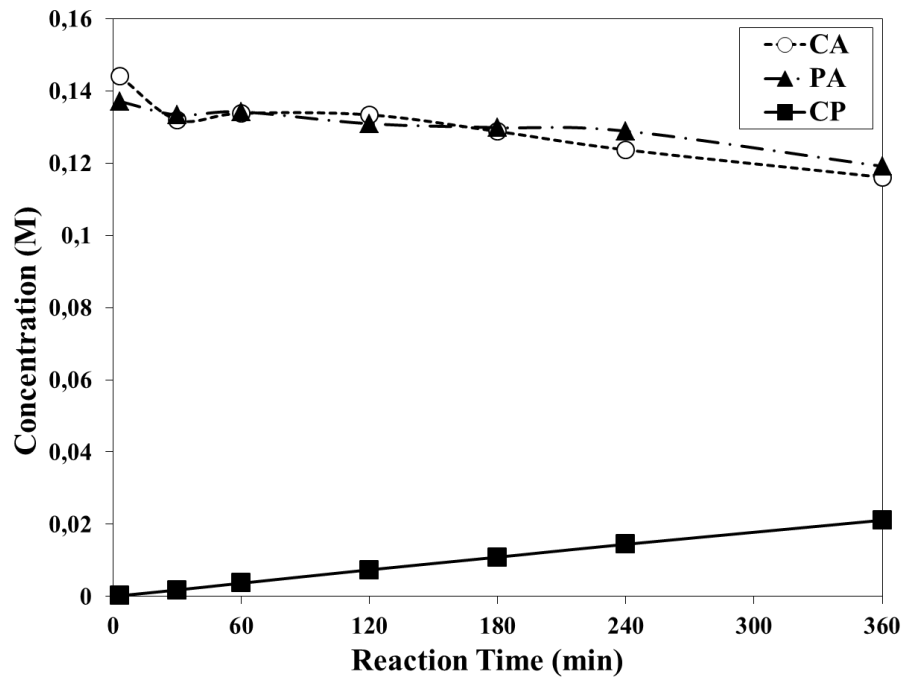

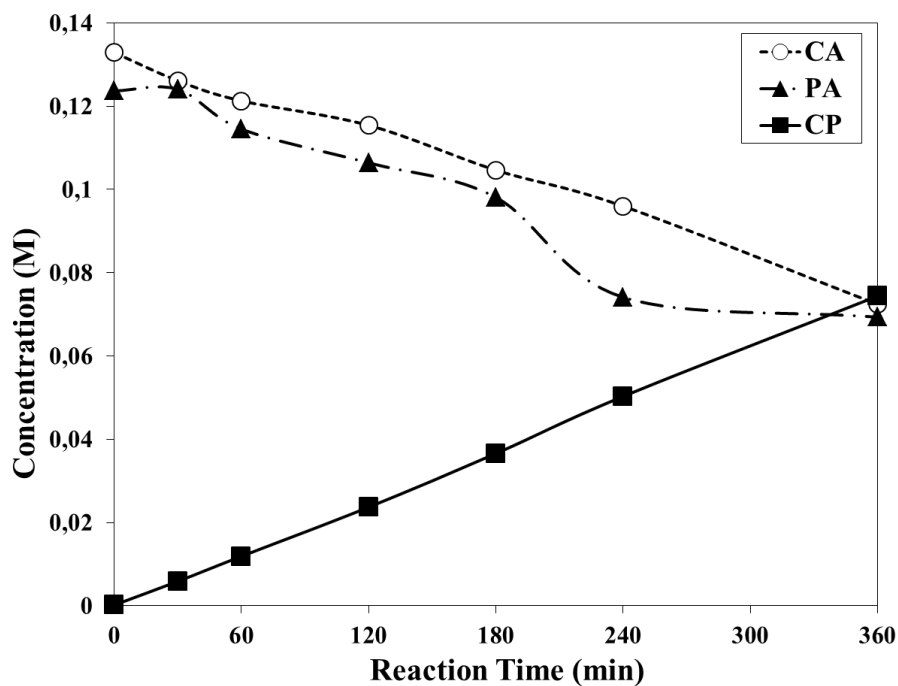Figure 5.18 The change in concentration reactants and product with time over 80 mg of WZSBA15-15-7

Figure 5.19. The change in concentration reactants and product with time over 160 mg of WZSBA15-15-7

Figure 5.20 shows the conversion obtained for different amounts of WZSBA15-15-7. The conversion rised significantly with the amount of catalysts.
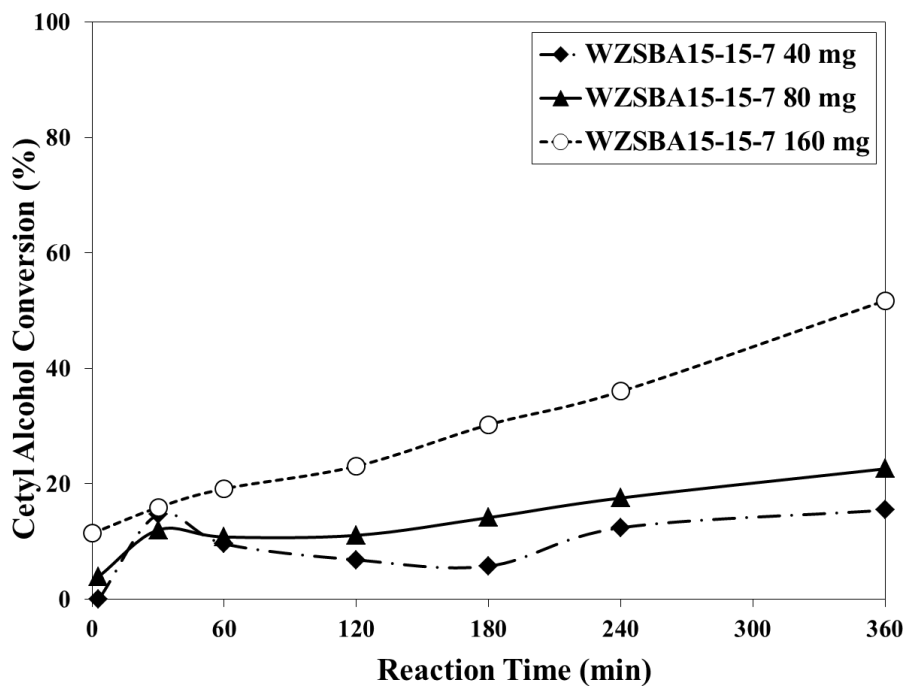

Figure 5.20. Conversion of cetyl alcohol over different amounts of WZSBA15-15-7

WZSBA15-15-8, WZSBA15-20-7, WZSBA15-20-8 and Zr-SBA-15 were tested under the same reaction conditions using 160 mg catalyst. The concentration change obtained over different catalysts are displayed in the Figure 5.21 to 5.24.
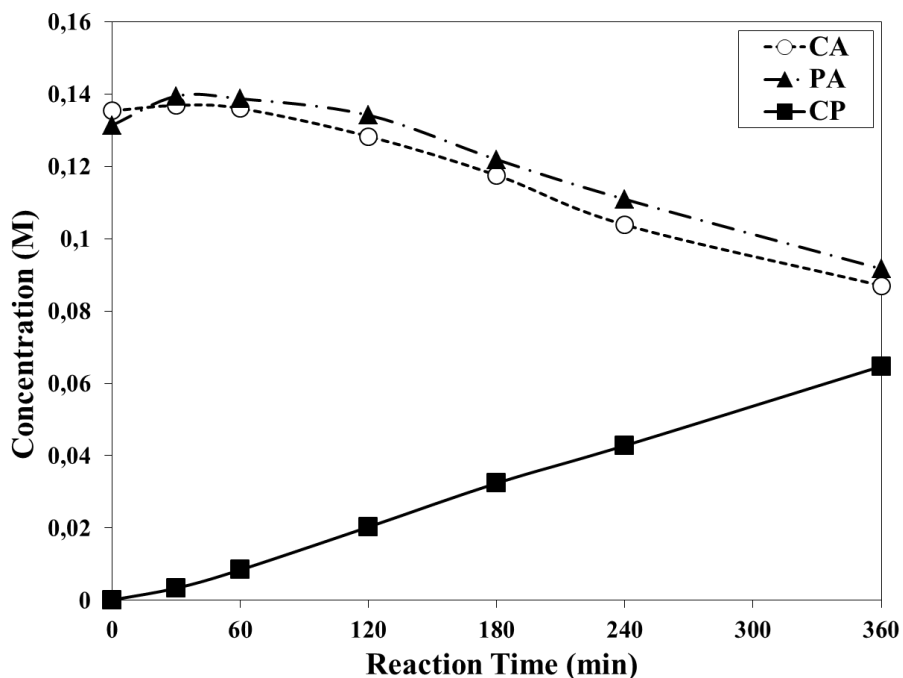

Figure 5.21. The change in concentration reactants and product with time over WZSBA15-15-8
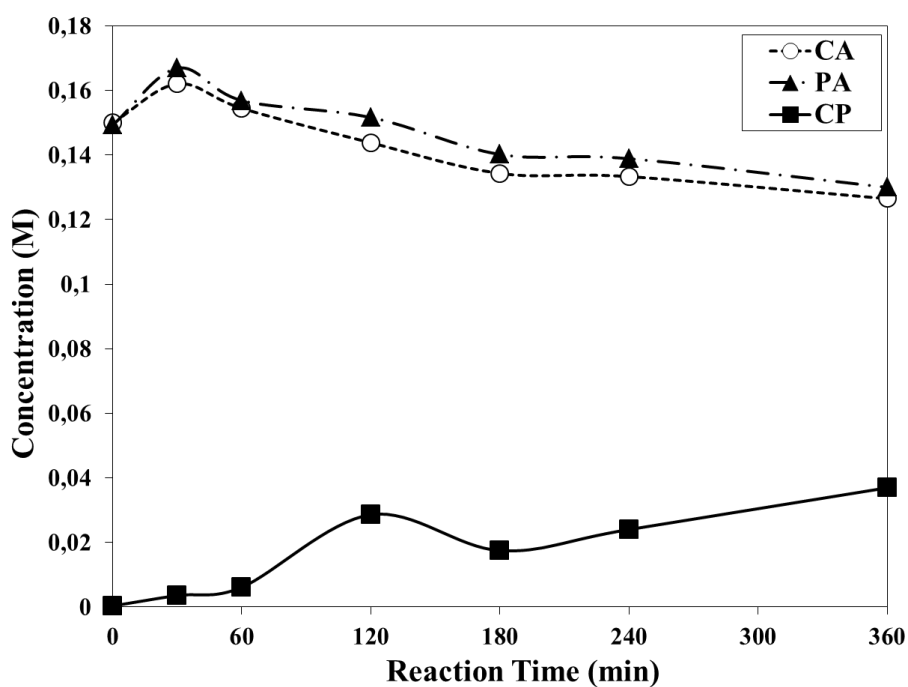

Figure 5.22. The change in concentration reactants and product with time over WZSBA15-20-7
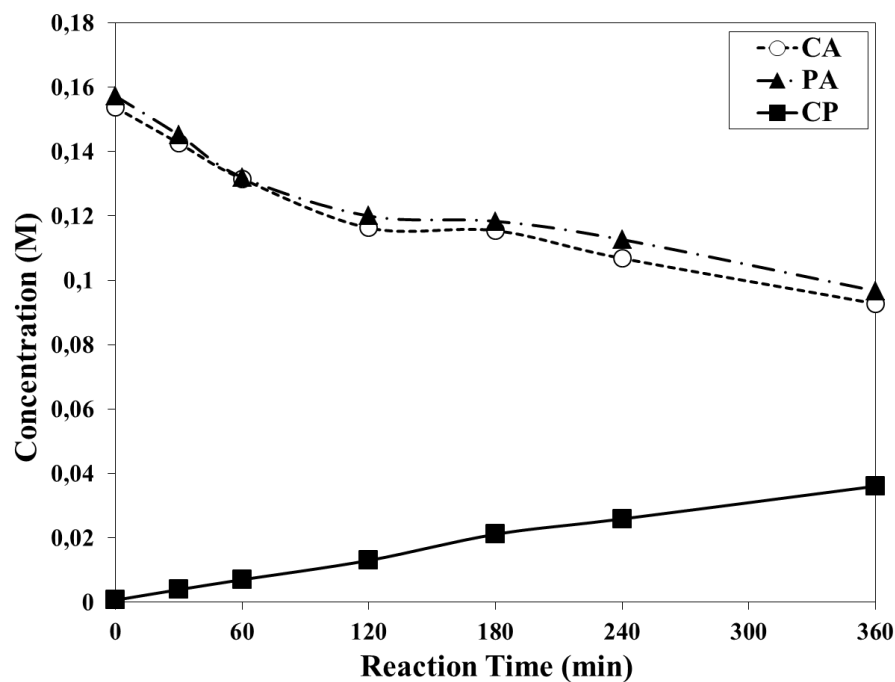
Figure 5.23. The change in concentration reactants and product with time over WZSBA15-20-8
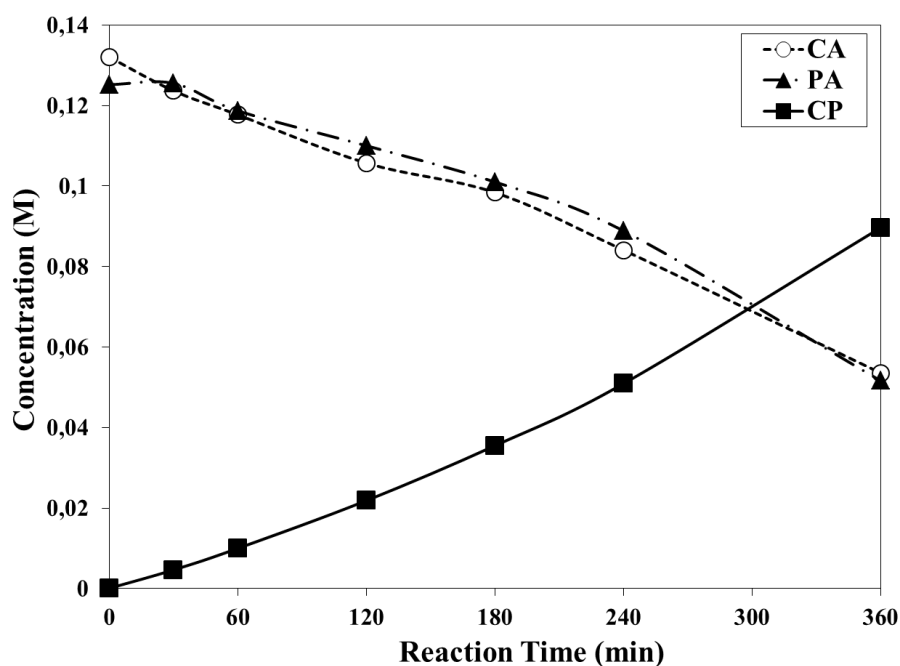

Figure 5.24. The change in concentration reactants and product with time over Zr-SBA-15

Cetyl palmitate was obtained as the only product over all catalysts. Figure 5.25 displays the conversion of cetyl alcohol obtained over different catalysts. Zr-SBA-15 gave the highest conversion within 6h reaction among the other catalysts. This might be caused by the high surface area and pore volume of Zr-SBA-15. When loading amount

of tungsten oxide was considered, the catalysts with 15 wt% loading of tungsten oxide gave higher conversions than the catalysts with 20 wt% loading for both calcination temperatures. This result also showed the importance of surface area and acidity of the catalyst for the high yield of esters. According to the characterization of the catalysts, increasing the loading amount of tungsten oxide, increased the amount of WO_3 crystals on the catalysts. The presence of WO_3 crystals had a decreasing effect on both the surface area and the acidity of the catalysts. The effect of calcination temperature on the activity of the catalyst could also be deduced from Figure 5.9. It was found from the characterizations that the acidity of the catalysts increased with calcination temperature. As a result of the increasing acidity, higher conversions were obtained over the catalysts calcined at 800 $^{\circ}$C.
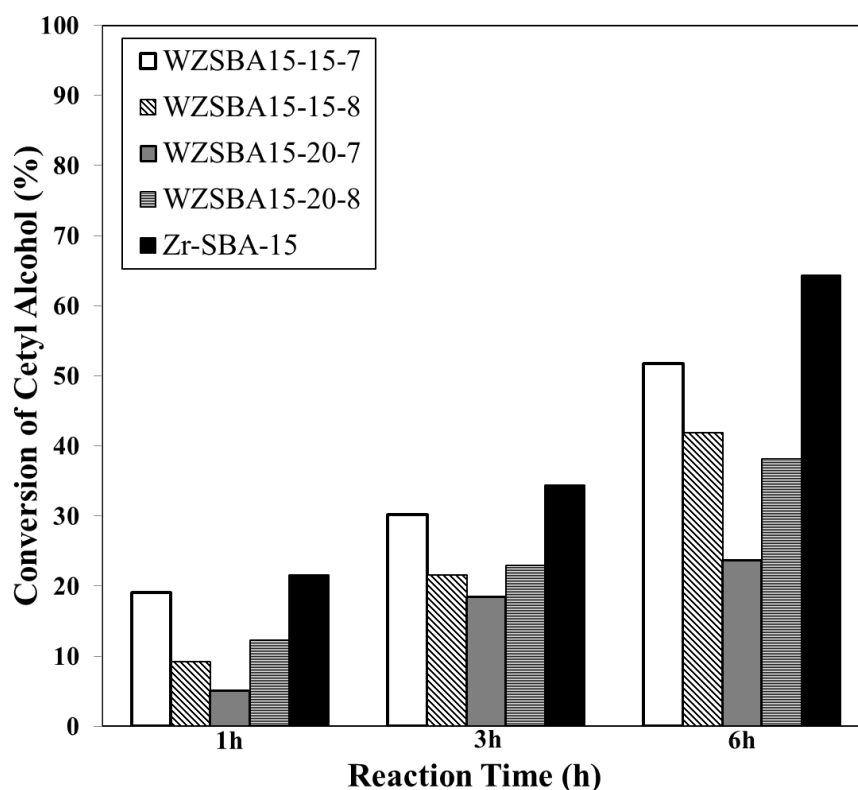

Figure 5.25. Cetyl alcohol conversion over different catalysts

The effect of excess cetyl alcohol amount (cetyl alcohol : palmitic acid mole ratio of 3:1) was investigated over the most active catalyst, Zr-SBA-15. The change in reactants and product distribution is given in Figure 5.26. Increasing the mole ratio did not have a significant effect on the yield of cetyl palmitate.
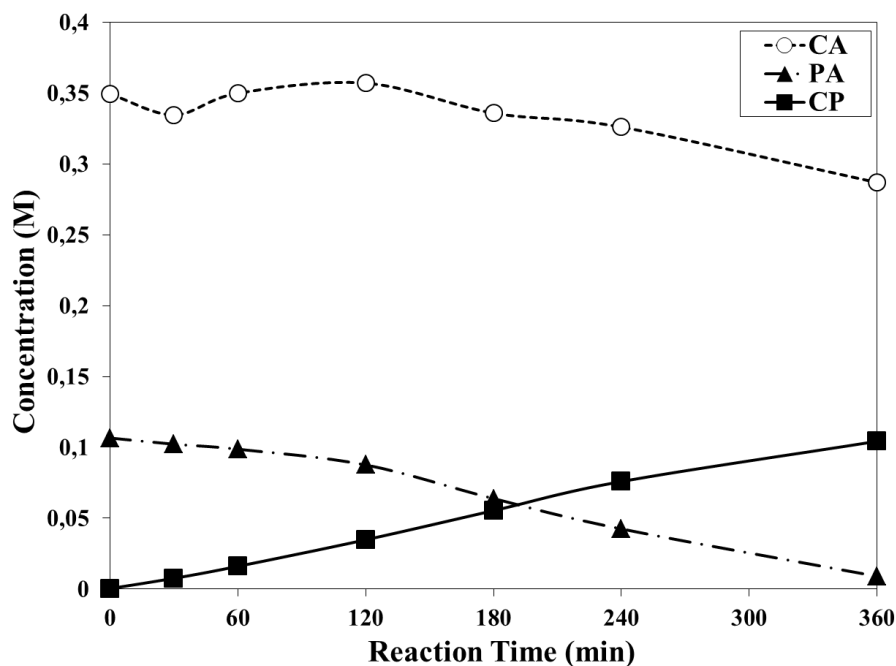
Figure 5.26. The change in concentration reactants and product with time over Zr-SBA-15 for CA:PA = 3:1

Elemental analysis of fresh and used Zr-SBA-15 was performed in order to investigate the leaching of the catalyst. The results of the analysis are given in Table 5.3. Zr content of the used catalyst was close to fresh catalyst. Therefore, it was deduced that the catalyst could be reused in the reaction.

This study was founded by TÜBİTAK as the project number 112M701. The studies will be continued with the different amount of Zr incorporation into SBA-15. Also zirconia and WO_3 will be loaded over SBA-15 by impregnation. The reusability tests will be performed with the catalys that give the best results.

CHAPTER 6

CONCLUSION

Tetragonal zirconia phase was obtained with high acidity for WO_3-ZrO_2 based catalysts (WZ15 and WZ20). The surface areas of the WZ15 and WZ20 catalysts were 81.3 and 87.8 m^2/g respectively as expected. Zr was incorporated into SBA-15 without destroying its structure and it provided the highest acidity among the catalysts investigated. Formation of WO_3 crystals were observed when WO_3 was loded onto Zr-SBA-15. WO_3 loading decresed the acidity, which was atributed to formation of WO_3 crystals. The amount of these crystals decreased with calcination temperature.

Cetyl palmitate was the only product formed in all the tests. Much higher conversions were obtained over the heteregenous catalyst compared to homegeneous one ($ZrOCl_2.8H_2O$). WZ20 gave the highest conversion (80 %), which was followed by Zr-SBA-15 based catalysts (64 %) . Higher activity was obtained with more acidic catalyst: Zr-SBA-15. This catalyst did not leach. Tungsten loaded Zr-SBA-15 catalysts showed lower activities. The increase in the calcination temperature resulted in an increase in the conversion, because it enhanced the acidity of the catalysts by lowering the amount of WO_3 crystals.However, catalyst activity was not affected by different WO_3 loading. Investigation of the effect of excess cetyl alcohol amount showed that the conversion did not effected by the reactant compositon significantly.

REFERENCES

Biswas, P; Narayanasarma, P; Kotikalapudi, C.M; Dalai, A.K; Adjaye, J; Characterization and activity of ZrO_2 doped SBA-15 supported NiMo catalysts for HDS and HDN of bitumen derived heavy gas oil. *Industrial & Engineering Chemistry Research*, 50, 2011, 7882-7895

Brahmkhatri, V; Patel, A; 12-Tungstophosphoric acid anchored to SBA-15: An efficient, enviromentally benign reusable catalysts for biodiesel production by esterification of free fatty acids. *Applied Catalysis A: General*, 403, 2011, 161-172

Fuxiang, L; Feng, Y; Yongli, L; Ruifeng, L; Kechang, X; Direct synthesis of Zr-SBA-15 mesoporous molecular sieves with high zirconium loading: characterization and catalytic performance after sulfated. *Microporous and Mesoporous Materials*, 101, 2007, 250-255

Gracia, M.D; Balu, A.M; Campelo, J.M; Luque, R; Marinas, J.M; Romero, A.A; Evidences of in situ generation of highly active Lewis acid species. *Applied Catalysis A:General*, 371, 2009, 85-91

Garg, S; Soni, K; Kumaran, G,M; Bal, R; Marek, K,G; Gupta, J,K; Sharma, L,D; Dhar, G,M; Acidity and catalytic activities of sulfated zirconia inside SBA-15. *Catalysis Today*, 14, 2009, 125-129

Ieda, N; Mantri, K; Miyata, Y; Ozaki, A; Komura , K; Sugi, Y; Esterification of long-chain acids and alcohols catalyzed by ferric chloride hexahydrate. *Ind. Eng. Chem. Res.*, 47, 2008, 8631-8638

Jiang, Y; Lu, J; Sun, K; Ma, L; Ding, J; Esterification of oleic acid with ethanol catalyzed by sulfonated cation exchange resin: Experimental and kinetic studies. *Energy Conversion and Management*, 76, 2013, 980-985

Mantri, K; Komura, K; Sugi, Y; ZrOCl2.8H2O catalysts for the esterification of long chain aliphatic carboxylic acids and alcohols. The enhancement of catalytic performance by supporting on ordered mesoporous silica. *Green Chemistry*, 2005, 7, 677-682

Mantri, K; Nakamura, R; Miyata, Y; Komura, K; Sugi, Y; Multi-valent salt hydrates as catalysts for the esterification of fatty acids and alcohols. *Material Science ForumVols*, 2007, 539-543

March, J; Smith, M.B; March's Advanced Organic Chemistry: Reactions, Mechanisms, and Structure. John Wiley & Sons, Seventh Edition, 2013

Marchetti, J.M; Errazu, A.M; Comparison of different heterogeneous catalysts and different alcohols for the esterification reaction of oleic acid. *Fuel*, 87, 2008, 3477-3480

Mayo, D,W; Pike, R,M; Forbes, D,C; Microscale Organic Laboratory: with Multistep and Multiscale Syntheses. John Wiley & Sons, Fifth Edition, 2010

Morales, I,J; Gonzalez, J,S; Torres, M; Lopez, A,J; Zirconium doped MCM-41 supported WO_3 solid acid catalysts for the esterification of oleic acid with methanol. *Applied Catalysis A:General*, 379, 2010, 61-68

Ni, J; Meunier, F.C; Esterification of free fatty acids in sunflower oil over solid acid catalysts using batch and fixed bed-reactors. *Applied Catalysis A: General*, 333, 2007, 122-130

Özbay, N; Oktar, N; Tapan, N.A; Esterification of free fatty acids in waste cooking oils (WCO): Role of ion-exchange resins. *Fuel*, 87, 2008, 1789-1798

Sakthivel, A ; Komura, K ; Sugi, Y; MCM-48 supported tungstophosphoric acid: an efficient catalyst for the esterification of long-chain fatty acids and alcohols in supercritical Carbon dioxide.

Santiesteban, J,G ; Vartuli, J,C ; Han, S ; Bastian, R,D ; Chang, C,D ; Influence of the Preparative Method on the Activity of Highly Acidic WOx/ZrO_2 and the Relative Acid Activity Compared with Zeolites. *Journal of Catalysis*, 168 ,1997, 431-441

Thielemann, J,P ; Girgsdies, F ; Schlögl, R ; Hess, C ; Pore structure and surface area of silica SBA-15: influence of washing and scale-up. *Brilstein Journal of Nanotechnology*, 2, 2011, 110-118

Vartuli, J,C ; Santiesteban, P ; Traverso, P ; Martinez, N,C; Chang, C,D ; Stevenson, S,A ; Characterization of the Acid Properties of Tungsten/Zirconia Catalysts Using Adsorption Microcalorimetry and n-Pentane Isomerization Activity. *Journal of Catalysis* ; 187, 1999, 131–138

Zhang, Y,Q ; Wang, S,J ; Wang, J, W ; Lou, L,L ; Zhang, C ; Liu, S ; Synthesis and characterization of Zr-SBA-15 supported tungsten oxide as a new mesoporous solid acid. *Solid State Sciences*, 11, 2009, 1412-1418

Zhang, C ; Liu, T ; Wang, H,J ; Wang, P ; Pan, X,Y ; Synthesis of acetyl salicylic acid over WO_3/ZrO_2 solid superacid catalyst. *Chemical Engineering Journal* , 174, 2011 236– 241

APPENDIX A
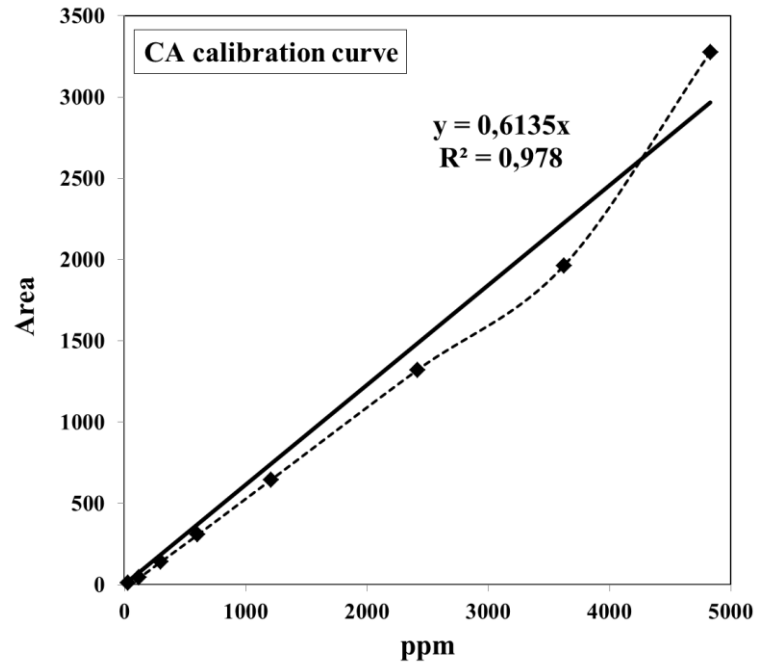
CALIBRATION CURVES OF GC STANDARDS

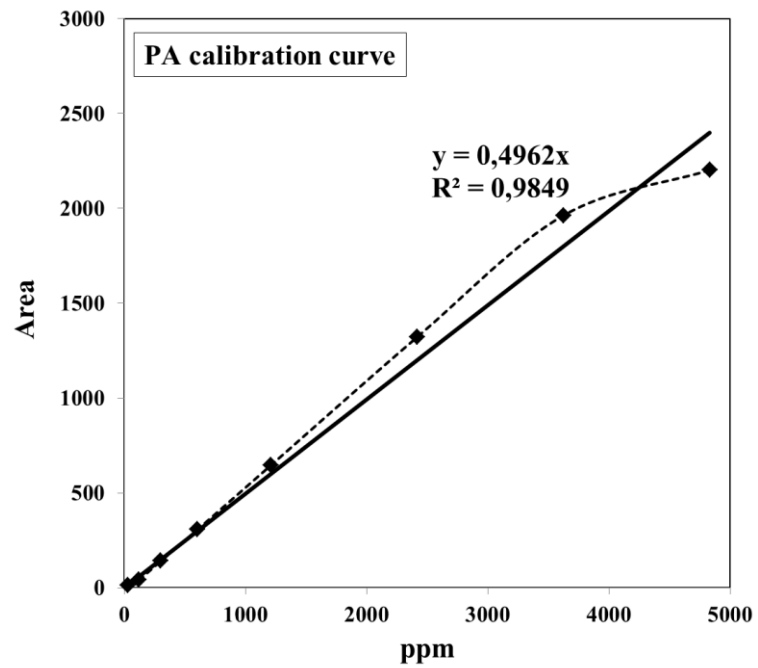Figure A.1. GC calibration curve for cetyl alcohol (CA)

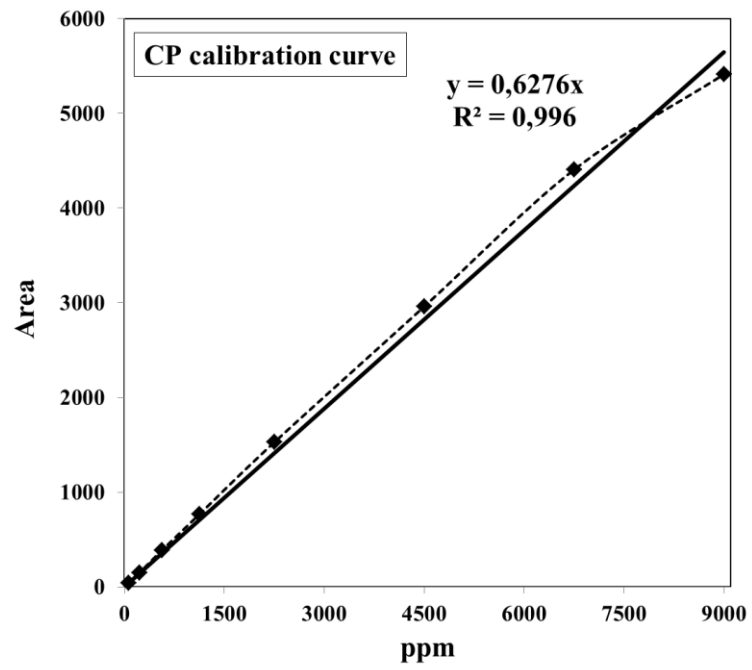

Figure A.2. GC calibration curve for palmitic acid (PA)

Figure A.3. GC calibration curve for palmitic acid (CP)